REPORT 1034

INVESTIGATION OF SPOILER AILERONS FOR USE AS SPEED BRAKES OR GLIDE-PATH CONTROLS ON TWO NACA 65-SERIES WINGS EQUIPPED WITH FULL-SPAN SLOTTED FLAPS [1]

By Jack Fischel and James M. Watson

SUMMARY

A wind-tunnel investigation was made to determine the characteristics of spoiler ailerons used as speed brakes or glide-path controls on an NACA 65-210 wing and an NACA 65₂-215 wing equipped with full-span slotted flaps. Several plug-aileron and retractable-aileron configurations were investigated on the two wing models with the full-span flaps retracted and deflected. Tests were made at various Mach numbers between 0.13 and 0.71.

The results of this investigation have indicated that the use of plug or retractable ailerons, either alone or in conjunction with wing flaps, as speed brakes or glide-path controls is feasible and very effective. In an illustrative example, the estimated time required for descent of a high-performance airplane from 40,000 feet was reduced from 12.3 minutes to 3.3 minutes. The plug and retractable ailerons investigated, when used as speed brakes, had only a small effect on the wing pitching moments. The rolling effectiveness of the ailerons will not be impaired by such use and should be as good as the effectiveness when the ailerons are projected in normal manner from the retracted position.

INTRODUCTION

One of the less obvious but nevertheless important needs of the high-performance military and commercial aircraft currently in use or in the design stage is that of utilizing suitable devices as aerodynamic speed brakes or glide-path controls, or both. Speed brakes and glide-path controls are beneficial for aircraft under various normal or emergency operating conditions, such as: a rapid descent from high altitude while airplane speed is being limited, landing on short runways over obstacles, reducing speed rapidly to increase the firing efficiency of fighter aircraft, and so forth. For the high-performance aircraft, the use of full-span slotted flaps and spoiler lateral-control devices would be particularly beneficial for providing high lift for landing and take-off as well as adequate lateral control. In order to obviate the necessity of including additional devices on the airplane, the use as speed brakes of spoiler ailerons, either alone or in conjunction with slotted flaps, was reported in reference 1 and was shown to be satisfactory. By means of suitable linkage, the slotted flaps can be deflected and the spoiler ailerons on both wing semispans can be projected equally above the wing to act as speed brakes or glide-path controls; and in either the neutral or an extended position, the ailerons can at the same time be operated differentially by movement of the control stick to provide lateral control.

The lateral control characteristics of various spoiler ailerons on unswept wings have been presented previously (for example, see references 2 to 7); however, the aerodynamic characteristics of these ailerons pertaining to their use as speed brakes or glide-path controls have seldom been presented.

In order to provide some information on the characteristics of plug and retractable ailerons when used as speed brakes or glide-path controls, the incremental values of lift, drag, and pitching-moment coefficients obtained at various aileron projections and flap deflections during the investigations of references 3 to 5 are presented herein. These data were obtained through a large angle-of-attack range on semispan wings having NACA 65-210 and NACA 65₂-215 airfoil sections. The investigation was performed in the Langley 7- by 10-foot tunnels at various Mach numbers between 0.13 and 0.71. Complete lift, drag, and pitching-moment data of these aforementioned wings with ailerons neutral have been presented in references 5 and 8. Data illustrating the rolling effectiveness of the ailerons when used as speed brakes or glide-path controls and a discussion pertaining to the application of the incremental lift, drag, and pitching-moment data to aircraft are presented herein.

COEFFICIENTS AND SYMBOLS

C_L lift coefficient $\left(\dfrac{\text{Twice lift of semispan model}}{qS}\right)$

C_D drag coefficient (D/qS)

C_m pitching-moment coefficient $(M_p/qS\bar{c})$

Δ increment caused by aileron projection

C_l rolling-moment coefficient (L/qSb)

c local wing chord, feet

$\bar{c}$ wing mean aerodynamic chord, 2.86 feet $\left(\dfrac{2}{S}\displaystyle\int_0^{b/2} c^2 dy\right)$

b twice span of each semispan model, 16 feet

y lateral distance from plane of symmetry, feet

S twice area of each semispan model, 44.42 square feet

D twice drag of semispan model, pounds

L rolling moment, resulting from aileron projection, about plane of symmetry, foot-pounds

M_p twice pitching moment of semispan model about 35-percent root-chord station

q free-stream dynamic pressure, pounds per square foot $\left(\frac{1}{2}\rho V^2\right)$

V free-stream velocity, feet per second

V_i indicated airspeed, miles per hour

ρ mass density of air, slugs per cubic foot

α angle of attack with respect to chord plane at root of model, degrees

δ_f flap deflection, measured between wing chord plane and flap chord plane (positive when trailing edge of flap is down), degrees

M Mach number (V/a)

R Reynolds number

a speed of sound, feet per second

CORRECTIONS

All data presented are based on the dimensions of each complete wing.

The test data have been corrected for jet-boundary effects according to the methods outlined in reference 9. The Glauert-Prandtl transformation (reference 10) has been utilized to account for effects of compressibility on these jet-boundary corrections. Blockage corrections were applied to the test data by the methods of reference 11.

MODEL AND APPARATUS

The right-semispan-wing models investigated with spoiler ailerons (figs. 1 to 6) were mounted in either the Langley 300 MPH 7- by 10-foot tunnel or the Langley high-speed 7- by 10-foot tunnel with their root sections adjacent to one of the vertical walls of the tunnel, the vertical wall thereby serving as a reflection plane. Two wings were used for this investigation: one wing embodied NACA 65–210 airfoil sections and the other wing embodied NACA 65_2–215 airfoil sections. The wings were constructed with the same plan-form dimensions (figs. 1, 3, and 5) and each wing had an aspect ratio of 5.76, a taper ratio of 0.57, and had neither twist nor dihedral. The NACA 65_2–215 wing was constructed with two trailing-edge sections which were used alternately for tests of the plain-wing configuration and for tests of the wing configuration with flaps (fig. 6). The NACA 65–210 wing was equipped with two trailing-edge sections—one to accommodate the basic plug-aileron and retractable-aileron configurations (fig. 2) and the other to accommodate the circular-plug-aileron configurations (fig. 4); each trailing-edge section had a cut-out to accommodate the flap in the retracted position ($\delta_f=0°$). A more detailed

description of the construction and mounting of the models is presented in references 3, 4, 5, and 8.

A 0.25c slotted flap which extended from the wing root section to the 95-percent-semispan station was used on both semispan wings in this investigation. This flap was originally designed and constructed to conform to the contour of the NACA 65–210 wing and was used in all investigations on that wing (references 3, 4, and 8). Because of its availability and satisfactory aerodynamic characteristics, this flap was also used in the flap-deflected wing configurations tested on the NACA 65_2–215 wing (reference 5). The positions of the flap with respect to the wing at the various deflections investigated with each aileron configuration are shown in figures 1, 3, and 6. These positions were found to be optimum, aerodynamically, for each flap deflection (references 5 and 8).

Each of the various aileron configurations investigated had a span of 49.2 percent of the wing semispan and was fabricated from duralumin or steel sheet in five equal spanwise segments (figs. 1 to 6). The basic plug ailerons and retractable ailerons on the NACA 65–210 wing had $\frac{5}{16}$-inch perforations which removed about 9 percent of the original aileron area (reference 3). On the NACA 65_2–215 wing, identical ailerons of varying projection were used in tests of both the plug-aileron and retractable-aileron configurations; these ailerons were fastened to the upper surface of the wing at the 0.70c station (fig. 6). Although these ailerons were not projected out of the wing profile (from the neutral position) as they would be in a practical airplane installation (for example, the configurations on the NACA 65–210 wing), the configurations investigated are believed to simulate practical airplane installations and to provide aerodynamic data representative of these installations. (See fig. 6.)

TESTS

All tests of the basic plug-aileron, the basic retractable-aileron, and the thin-plate circular-plug-aileron configurations on the NACA 65–210 wing model were performed in the Langley high-speed 7- by 10-foot tunnel. All tests of the double-wall circular-plug-aileron configuration on the NACA 65–210 wing model and of the two aileron configurations on the NACA 65_2–215 wing model were performed in the Langley 300 MPH 7- by 10-foot tunnel.

With the flap retracted or deflected, the aerodynamic characteristics of each wing-aileron configuration were determined at various aileron projections and for several angles of attack. Tests were made at Mach numbers between 0.13 and 0.71 (with corresponding Reynolds numbers of 2.6×10^6 to 11.6×10^6, based on the wing mean aerodynamic chord of 2.86 ft). Negative aileron projections indicate that the ailerons were extended above the wing upper surface.

The average variation of Reynolds number with Mach number for all tests is shown in figure 7.

RESULTS AND DISCUSSION

EFFECT OF AILERON BRAKES ON WING AERODYNAMIC CHARACTERISTICS

Incremental data of lift, drag, and pitching-moment coefficients obtained at various aileron projections with the four aileron configurations investigated on the NACA 65–210 wing and with the flap retracted and deflected are presented in figures 8 to 15. Corresponding data obtained with the two aileron configurations on the NACA 65$_2$–215 wing are presented in figures 16 to 23.

Incremental lift coefficient ΔC_L.—The incremental values of lift coefficient generally became more negative with increase in aileron projection for all aileron configurations and flap conditions. The data obtained with the basic retractable aileron, however, showed inconsistent trends of reversed or positive values of ΔC_L for small aileron projections at various angles of attack and Mach numbers with the flap deflected. (See figs. 11, 22, and 23.) This phenomenon is usually exhibited by retractable ailerons with the flap deflected. A comparison of the present data with the rolling-moment data of references 3 to 5 shows, as anticipated, that the aforementioned effects paralleled the rolling effectiveness of the ailerons; that is, the rolling effectiveness increased when ΔC_L became more negative.

In general, the incremental values of lift coefficient increased negatively with increases in the Mach and Reynolds numbers and with increase in the flap deflection for all configurations. In most cases, increases in the angle of attack produced a small or inconsistent effect on the values of ΔC_L produced by almost all the ailerons; the thin-plate circular-plug aileron on the NACA 65–210 wing was the only configuration for which ΔC_L became more negative with increased angle of attack (figs. 12 and 13).

The plug ailerons on both wings usually produced slightly larger negative values of ΔC_L than the retractable ailerons. This effect is consistent with the fact that the rolling effectiveness usually observed for the plug aileron is greater than that for the retractable aileron (references 3 and 5). A comparison of the plug-aileron and retractable-aileron data obtained on the two wings alsoi shows that more negative values of ΔC_L were generally obta ned on the thicker wing. (See figs. 8 to 11, 16, 19, 20, and 23.)

Incremental drag coefficient ΔC_D.—The incremental drag data of figures 8 to 23—which are based on the values of drag coefficient measured on the wings at approximately a constant angle of attack (at the values of α and C_L shown in the figures for zero aileron projection)—exhibit certain trends that accompanied the lift changes discussed in the section entitled "Incremental lift coefficient ΔC_L." In most cases, the incremental values of drag coefficient increased with increase in aileron projection; however, at large values of lift coefficient with the flap deflected, an opposite trend was exhibited over a part of the projection range. The values of ΔC_D exhibited a negligible or inconsistent variation with increase in Mach and Reynolds numbers, except possibly at low negative values of C_L with flap retracted (figs. 8 and 10).

In general, the values of ΔC_D became considerably larger (or more positive) as the flap was deflected at a constant value of lift coefficient; however, an increase in the angle of attack and lift coefficient in any flap configuration generally caused a decrease in the values of ΔC_D. This decrease in ΔC_D became more pronounced with increase in aileron projection and with deflection of the flap and, in some instances, particularly at the higher lift coefficients with the flap deflected, the values of ΔC_D became negative. An analysis of the data shows that these trends result from the smaller positive increment in profile drag and the larger reduction in induced wing drag produced by projection of the ailerons as the angle of attack and lift coefficient increased.

For all practical purposes, however, some of the aforementioned changes in ΔC_D—particularly the decreases in the values of ΔC_D with increase in C_L, and the negative values of ΔC_D—would probably never be realized by an airplane in flight. The loss in lift resulting from projection of the aileron brakes on the airplane would probably have to be restored by an increase in the wing angle of attack to retain constant lift and avoid excessive accelerations and sinking speeds. This increase would result in approximately a constant induced drag and an increase in the total wing drag because of the larger profile drag resulting from the higher wing angle of attack and the projected aileron brakes. In order to illustrate the changes in ΔC_D obtained at constant lift coefficient for various aileron projections over the lift-coefficient range, some of the data of figures 8 to 23 have been analyzed and plotted as shown in figure 24. The values of ΔC_D resulting from aileron projection, with angle of attack varied to maintain constant lift coefficient, increased with increase in aileron projection and flap deflection and, for a given aileron projection, ΔC_D was usually fairly constant over the lift-coefficient range. In addition, the incremental drag values were negligibly affected by changes in Mach and Reynolds numbers.

The plug and retractable ailerons produced approximately similar values of ΔC_D on each wing model, but the two circular-plug ailerons generally produced the highest values of ΔC_D on the NACA 65–210 wing model. The data also show that more positive values of ΔC_D were usually obtained on the NACA 65$_2$–215 wing than on the NACA 65–210 wing at corresponding aileron projections and lift coefficients; however, the large changes in ΔC_D observed for the plug ailerons on the NACA 65$_2$–215 wing at small projections (figs. 16 to 19, and 24) result principally from the sudden opening of the plug slot rather than from the projection of the aileron alone, as was discussed for the lateral-control investigation reported in reference 5.

Incremental pitching-moment coefficient ΔC_m.—In general, the values of ΔC_m obtained at various aileron projections became more negative (or less positive) with increase in angle of attack in all flap conditions and became more negative with increase in aileron projection in the flap-retracted condition. Changes in the Mach and Reynolds

numbers generally had a negligible or an inconsistent effect on the values of ΔC_m obtained in all flap conditions, and the values of ΔC_m usually became less negative (or more positive) with increase in flap deflection. Because all values of ΔC_m were fairly small, however, the incremental wing pitching moments would probably be easily trimmed on an airplane, regardless of flap condition or aileron configuration.

EFFECT OF AILERON BRAKES ON AIRCRAFT PERFORMANCE

In order to illustrate the utility and one of the advantages to be gained from the changes in lift and drag produced by spoiler ailerons when used as glide-path controls on an airplane, the descent characteristics from an altitude of 40,000 feet of a typical high-performance airplane with and without glide-path controls were computed and are presented in figure 25. Unpublished wind-tunnel data obtained on the model of a high-performance propeller-driven airplane having four engines were used to determine the characteristics of the basic airplane. This airplane had a wing loading of 63 pounds per square foot, a wing aspect ratio of 10.18, and a wing taper ratio of 0.43; in addition, an effective thrust of zero in the flap-retracted condition was assumed. The glide-path controls assumed for the airplane were plug ailerons projected 8 percent chord above both wing panels, and the incremental data used for the glide-path controls were taken from data obtained on the NACA 65_2–215 wing (fig. 16). Although the NACA 65_2–215 wing had a lower aspect ratio than that of the assumed airplane, the lift coefficients at which the assumed airplane flew, in the illustrative example, were low enough to minimize differences in the induced drag and, hence, the incremental drag resulting from aileron projection. For other cases, however, particularly at high lift coefficients, differences in aspect ratio may cause appreciable drag differences which should be considered in a performance analysis. The airplane descent was assumed to start at an altitude of 40,000 feet and a Mach number of 0.7, and the airplane maintained this Mach number until an indicated airspeed of 450 miles per hour was reached. This indicated airspeed was then maintained for the remainder of the descent to sea level.

As can be seen from figure 25, projection of the plug aileron on both wing panels of the airplane decreased the time required to descend from 40,000 feet to sea level from 12.3 to 3.3 minutes. Also a decrease in the horizontal distance required to reach sea level of approximately 73 miles was effected (a straight line of descent was assumed). This saving of time and distance in descending from high altitudes would be particularly important for an emergency condition, such as failure in the cabin pressurization, and also for normal operating conditions, such as at the termination of a long-distance flight at the most efficient altitude (reference 12).

The illustrative example presented in the foregoing discussion was computed with the assumption that the airplane angle of attack was varied to maintain the proper lift coefficient with the flap retracted. This method of operation, however, may not be the most effective one. Deflection of the flap and ailerons simultaneously to provide the necessary lift coefficient at a constant angle of attack—and, at the same time, to increase the drag—or deflection of the ailerons with

the flaps deflected may result in larger decreases in the time and distance required to reach sea level than are shown in the illustrative example. However, other problems, such as downwash fluctuations in the region of the tail plane and excessive flap loads possibly encountered at high Mach number, may complicate or prevent such means of operation. For the illustrative example (wherein a −8-percent-chord aileron projection was employed), in order to maintain a constant α approximately a 10° deflection of the full-span flap would probably be required for simultaneous operation of flap and ailerons as glide-path controls. In general, the simultaneous use of the flaps and the aileron brakes will probably depend on the variation of lift and pitching moment desired for particular maneuvers, such as fighter combat maneuvers, in which only a drag increment is desired.

In addition to their action as glide-path controls, spoiler-aileron brakes provide the added advantage of decreasing wing bending moments by moving the spanwise center of loading inboard on the wings, as shown in figure 26. This effect is particularly important and beneficial for airplanes during descent at high speeds and lessens the possibility of structural failure during this maneuver.

Projection of the ailerons with the flaps deflected in a landing approach would also substantially aid the airplane in landing over high obstacles and on short landing fields and would appreciably decrease the length of landing run. The use of spoiler ailerons as speed brakes to limit or reduce airplane speed in a dive or to reduce airplane speed rapidly in order to increase firing efficiency of fighter aircraft is also feasible, as is apparent from the data previously presented.

Another functional advantage obtainable with spoiler-aileron brakes is the possible use of the ailerons as a gust-alleviation device. Because of the relatively greater adverse effects on passenger riding comfort and wing structural loads of gusts at high speeds, an automatic spoiler-aileron gust-alleviation system should be given due consideration.

Although a comparison of the characteristics of the spoiler-aileron speed brakes discussed herein with the characteristics of other brake devices (such as those of references 13 to 15) is not presented, several advantages of the aileron brakes are readily apparent. These advantages include: The variable braking control permitted by the aileron brakes as compared with the inflexibility of control of some of the other devices; the use of spoiler-aileron brakes would obviate the necessity of including separate braking devices on an airplane; the aileron brakes may be used, retracted into the wing, and immediately used again, but a parachute brake can be used only once before disposal or repacking (on the ground) and is inflexible in control; and also, the spoiler-aileron device would not adversely affect the effectiveness of adjoining wing controls, whereas other devices may (reference 15). In addition, unlike reversible-pitch propeller brakes (reference 16), spoiler-aileron brakes may be used on aircraft having diverse propulsive systems and would obviate any complexity involved in the use of propeller brakes on conventionally powered aircraft. The projected ailerons, when used as glide-path controls or speed brakes, probably would not cause severe tail buffeting inasmuch as the ailerons are placed on the outboard part of the wing near the tip, and the

wake formed by them would be outboard of the tail surfaces. Few data are available, however, concerning any induced effects of the aileron brakes on the wing downwash or on fluctuations in the downwash, and further investigation of such effects may be desirable.

ROLLING CHARACTERISTICS OF THE SPOILER AILERONS USED AS SPEED BRAKES OR GLIDE-PATH CONTROLS

In references 3 to 5, the rolling effectiveness of the plug and retractable ailerons on the NACA 65–210 and NACA 65₂–215 wings was shown to be very satisfactory for normal operation from the retracted aileron position. In order to illustrate the rolling effectiveness of these ailerons from a projected position—that is, when they are used as glide-path controls or speed brakes—some of the data previously presented in references 3 to 5 have been replotted, with zero rolling moment corresponding to some finite aileron projection on both semispans of a complete wing, and are presented in figures 27 to 29. The values of lift coefficient and angle of attack listed on these figures are those obtained with the ailerons in the raised position on both wing panels.

These data indicate that the rolling effectiveness produced by the plug and retractable ailerons from a projected-aileron neutral position was very satisfactory, particularly for the flap-deflected condition. For normal operation from the retracted aileron position, an aileron control-stick differential providing approximately equal up and down projections will probably be required for the plug ailerons; whereas a differential providing large up projections and little or no down projections for lateral control may be required for the retractable ailerons. However, when the ailerons are also used as speed brakes and glide-path controls, any extreme aileron control-stick differential normally employed for lateral control (such as that for the retractable ailerons) would probably have to change as the brakes project on both semispan wings, so that an aileron control-stick linkage allowing approximately equal up and down projections would be obtained for moderate brake projections on both wing panels.

CONCLUSIONS

A wind-tunnel investigation was made to determine the characteristics of plug and retractable ailerons used as speed brakes or glide-path controls on an NACA 65–210 and an NACA 65₂–215 wing equipped with full-span slotted flaps. The investigation was performed at various Mach numbers from 0.13 to 0.71. The results of the investigation led to the following conclusions:

1. The time for descent and distance for descent from high altitudes and wing bending moments can be greatly reduced by use of spoiler ailerons as brakes.

2. When used as speed brakes or glide-path controls, the rolling effectiveness of plug and retractable ailerons need not be impaired as compared with the effectiveness of the ailerons from the fully retracted position.

3. The incremental values of drag coefficient ΔC_D produced by projection of the ailerons on both wing panels of a complete wing generally became more positive with increase in aileron projection and flap deflection and were inconsistently or negligibly affected by changes in Mach

number. In addition, the ailerons generally produced larger increments of drag on the thicker wing model.

4. The increment in lift coefficient ΔC_L produced by projection of the ailerons generally became more negative with increase in aileron projection, flap deflection, and Mach and Reynolds numbers.

5. In general, the incremental values of pitching-moment coefficient ΔC_m produced by projection of the ailerons were fairly small, varied only slightly with changes in angle of attack, Mach number, aileron projection, or flap deflection and were about the same on both wing models.

LANGLEY AERONAUTICAL LABORATORY,
 NATIONAL ADVISORY COMMITTEE FOR AERONAUTICS,
  LANGLEY FIELD, VA., *June 3, 1949.*

REFERENCES

1. Rogallo, F. M.: Aerodynamic Characteristics of a Slot-Lip Aileron and Slotted Flap for Dive Brakes. NACA ACR, April 1941.
2. Fischel, Jack, and Ivey, Margaret F.: Collection of Test Data for Lateral Control with Full-Span Flaps. NACA TN 1404, 1948.
3. Fischel, Jack, and Schneiter, Leslie E.: High-Speed Wind-Tunnel Investigation of an NACA 65–210 Semispan Wing Equipped with Plug and Retractable Ailerons and a Full-Span Slotted Flap. NACA TN 1663, 1948.
4. Fischel, Jack: Wind-Tunnel Investigation of an NACA 65–210 Semispan Wing Equipped with Circular Plug Ailerons and a Full-Span Slotted Flap. NACA TN 1802, 1949.
5. Fischel, Jack, and Vogler, Raymond D.: High-Lift and Lateral Control Characteristics of an NACA 65₂–215 Semispan Wing Equipped with Plug and Retractable Ailerons and a Full-Span Slotted Flap. NACA TN 1872, 1949.
6. Deters, Owen J., and Russell, Robert T.: Investigation of a Spoiler-Type Lateral Control System on a Wing with Full-Span Flaps in the Langley 19-Foot Pressure Tunnel. NACA TN 1409, 1947.
7. Fischel, Jack, and Tamburello, Vito: Investigation of Effect of Span, Spanwise Location, and Chordwise Location of Spoilers on Lateral Control Characteristics of a Tapered Wing. NACA TN 1294, 1947.
8. Fischel, Jack, and Schneiter, Leslie E.: High-Speed Wind-Tunnel Investigation of High Lift and Aileron-Control Characteristics of an NACA 65–210 Semispan Wing. NACA TN 1473, 1947.
9. Swanson, Robert S., and Toll, Thomas A.: Jet-Boundary Corrections for Reflection-Plane Models in Rectangular Wind Tunnels. NACA Rep. 770, 1943.
10. Göethert, B.: Plane and Three-Dimensional Flow at High Subsonic Speeds. NACA TM 1105, 1946.
11. Thom, A.: Blockage Corrections in a Closed High-Speed Tunnel. R. & M. No. 2033, British A.R.C., 1943.
12. Shevell, Richard S.: Operational Aerodynamics of High-Speed Transport Aircraft. Jour. Aero. Sci., vol. 15, no. 3, March 1948, pp. 133–143.
13. Purser, Paul E., and Turner, Thomas R.: Wind-Tunnel Investigation of Perforated Split Flaps for Use as Dive Brakes on a Tapered NACA 23012 Airfoil. NACA ARR, Nov. 1941.
14. Purser, Paul E., and Turner, Thomas R.: Aerodynamic Characteristics and Flap Loads of Perforated Double Split Flaps on a Rectangular NACA 23012 Airfoil. NACA ARR, Jan. 1943.
15. Toll, Thomas A., and Ivey, Margaret F.: Wind-Tunnel Investigation of a Rectangular NACA 2212 Airfoil with Semispan Ailerons and with Nonperforated, Balanced Double Split Flaps for Use as Aerodynamic Brakes. NACA ARR L5B17, 1945.
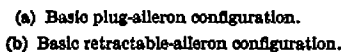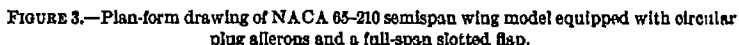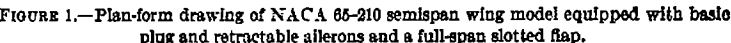16. Stone, Irving: Reversible Props Brake Plane in Dive. Aviation Week, Dec. 27, 1948, pp. 22 and 25.

FIGURE 1.—Plan-form drawing of NACA 65–210 semispan wing model equipped with basic plug and retractable ailerons and a full-span slotted flap.

FIGURE 3.—Plan-form drawing of NACA 65–210 semispan wing model equipped with circular plug ailerons and a full-span slotted flap.

(a) Basic plug-aileron configuration.

(b) Basic retractable-aileron configuration.

FIGURE 2.—Section drawings of basic plug-aileron and retractable-aileron configurations investigated on NACA 65–210 wing model.

(a) Thin-plate circular-plug-aileron configuration.

(b) Double-wall circular-plug-aileron configuration.

FIGURE 4.—Section drawings of thin-plate and double-wall circular-plug-aileron configurations investigated on NACA 65–210 wing model.
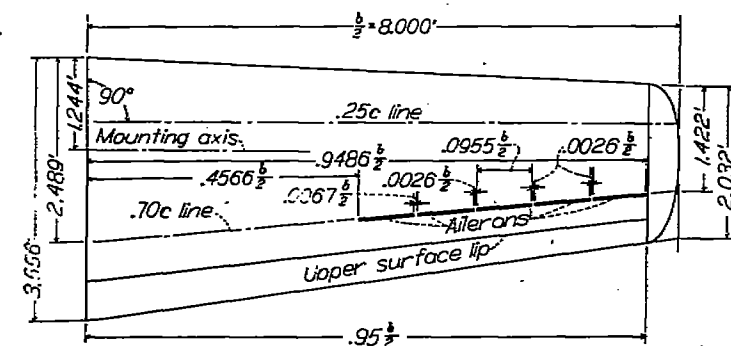
FIGURE 5.—Plan-form drawing of NACA 65₁-215 semispan wing model equipped with plug and retractable ailerons and a full-span slotted flap.
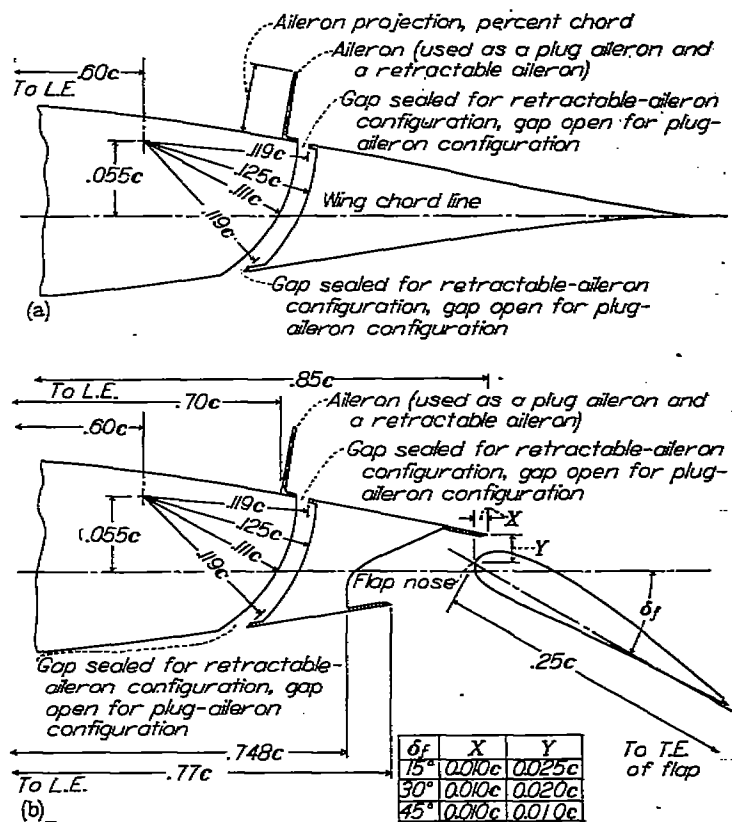
(a) Aileron configuration on the plain wing.

(b) Aileron configuration with flap deflected.

FIGURE 6.—Section drawings of plug-aileron and retractable-aileron configurations investigated on NACA 65₁-215 wing model.
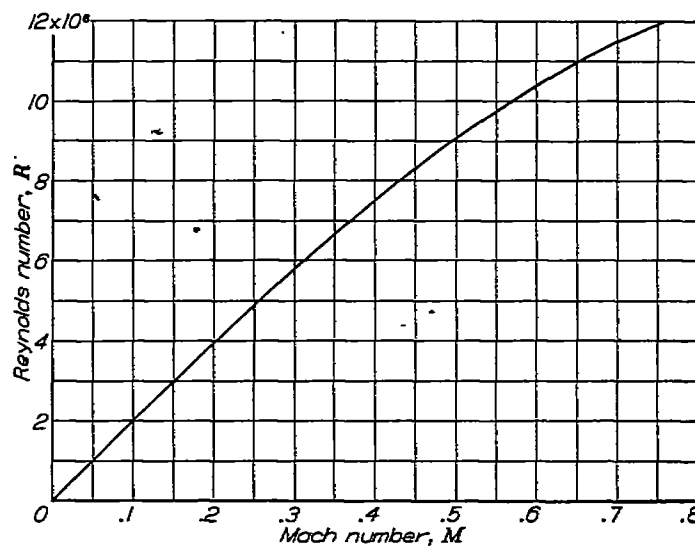
FIGURE 7.—Average variation of Reynolds number with Mach number. Reynolds number is based on wing mean aerodynamic chord of 2.86 feet.
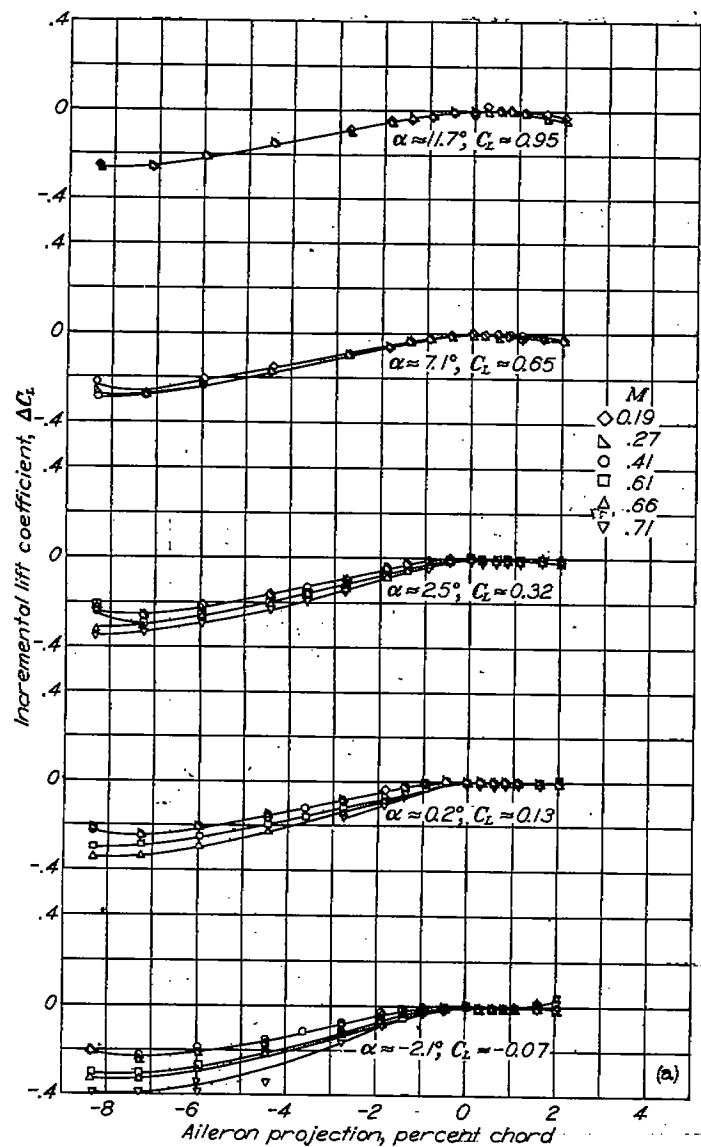
FIGURE 8.—Incremental values of lift, drag, and pitching-moment coefficients obtained by projection of the basic plug aileron on both semispans of the NACA 65-210 wing. Flap retracted.
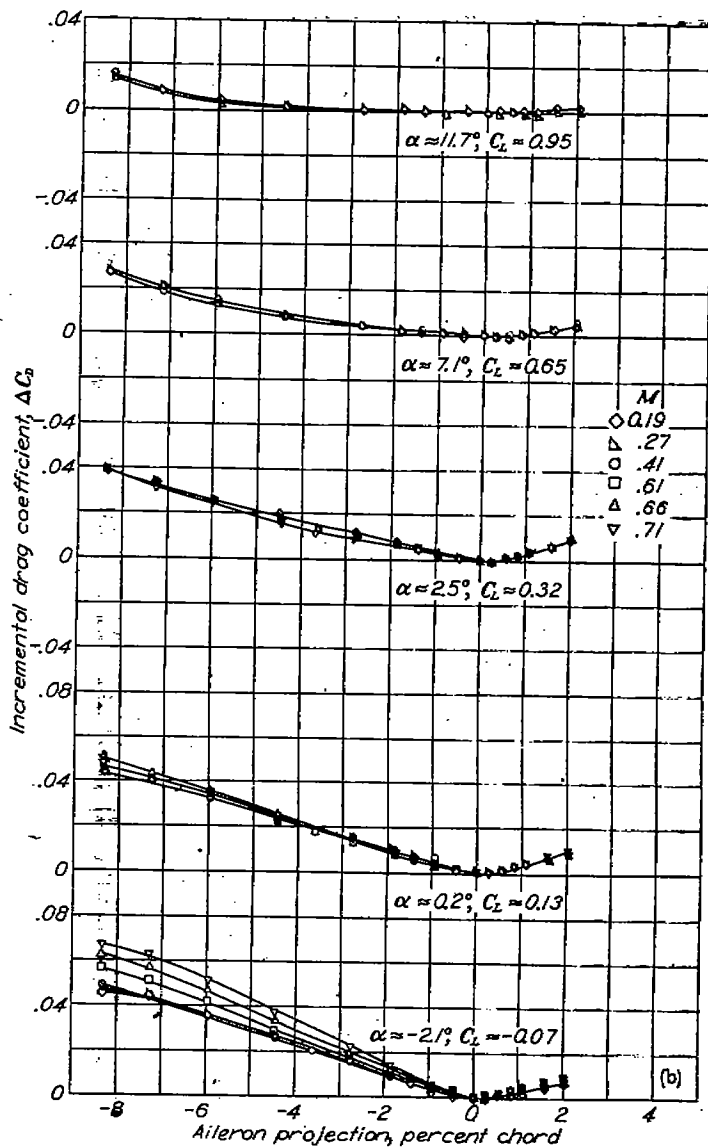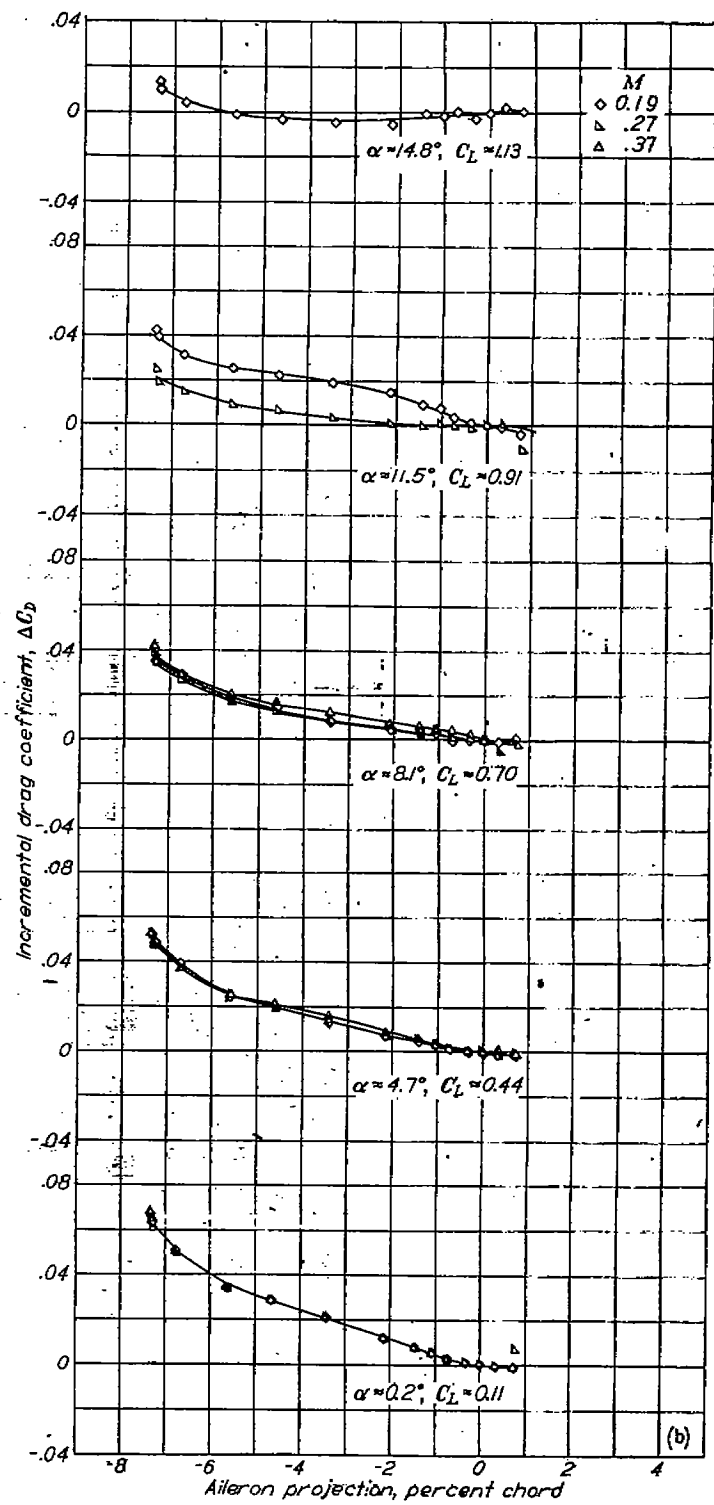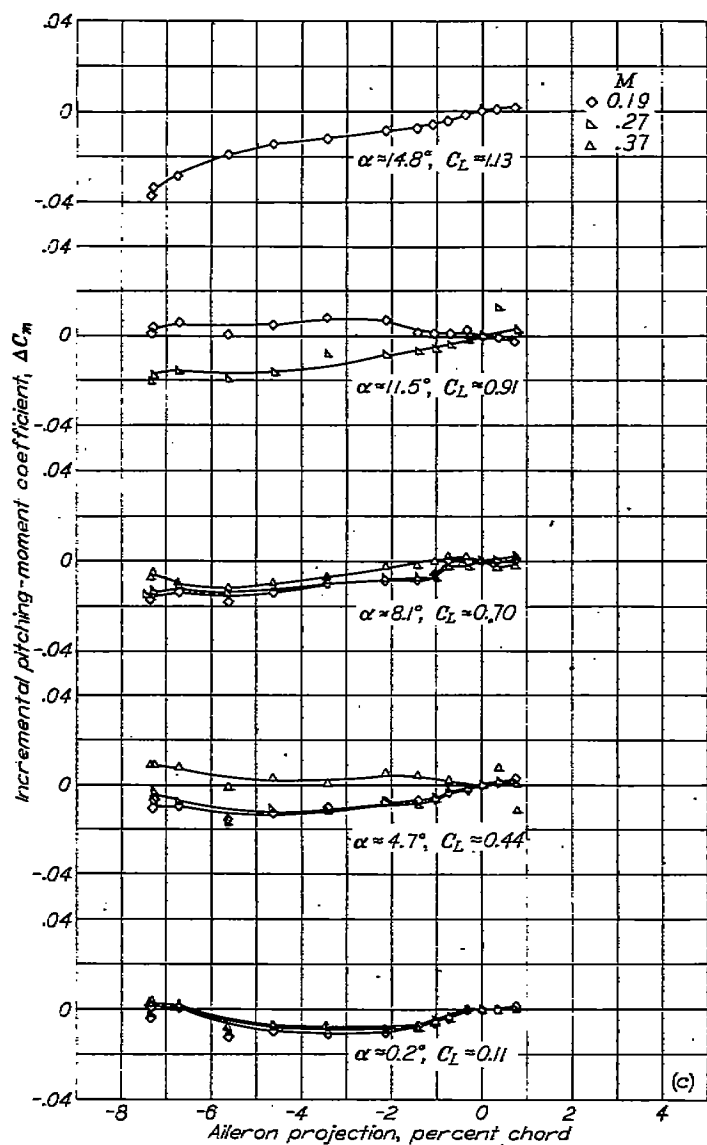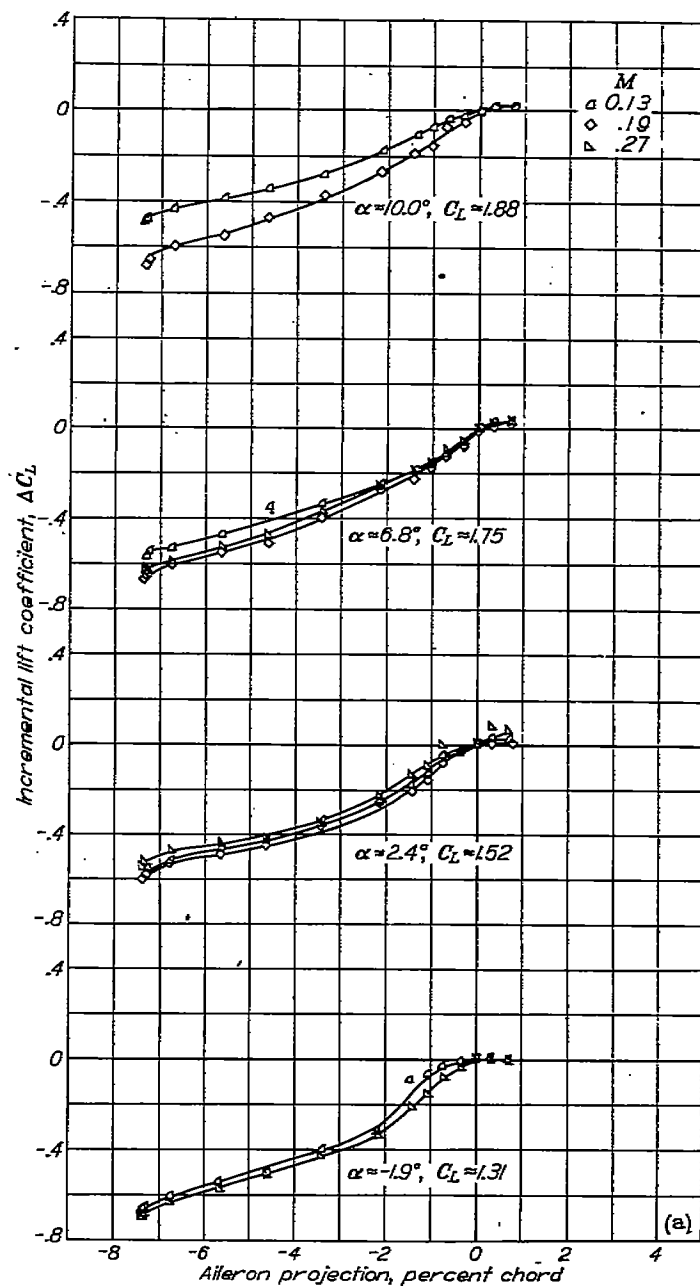
FIGURE 8.—Continued.
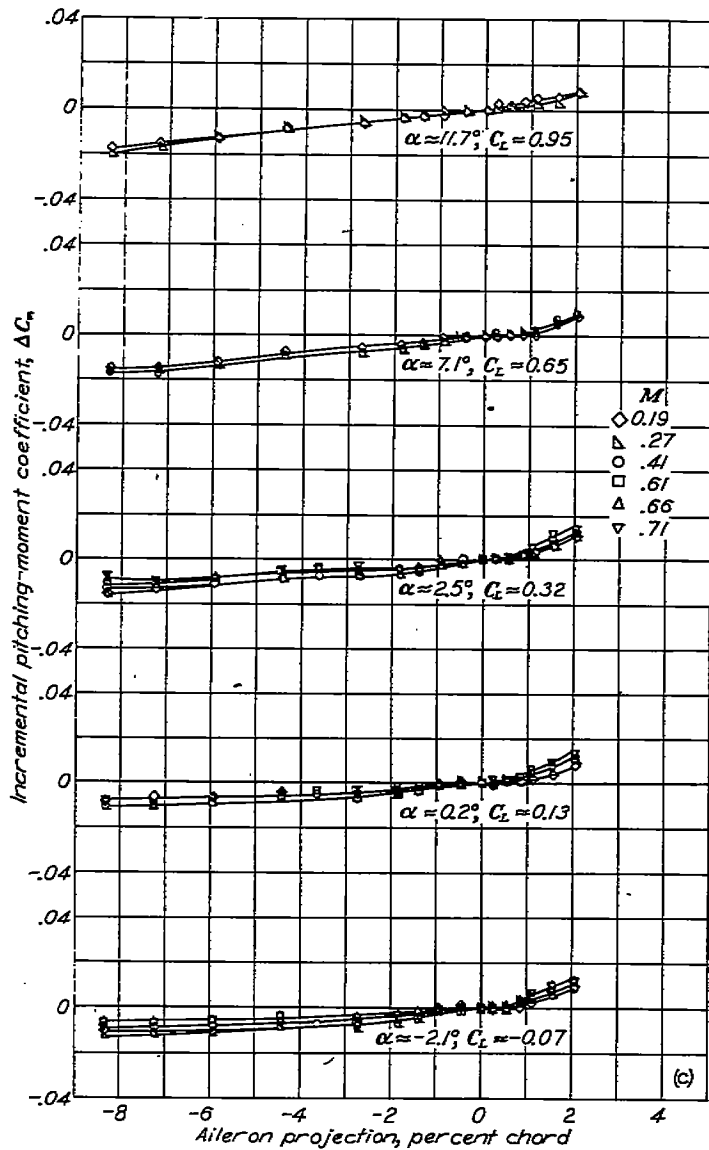
FIGURE 8.—Concluded.
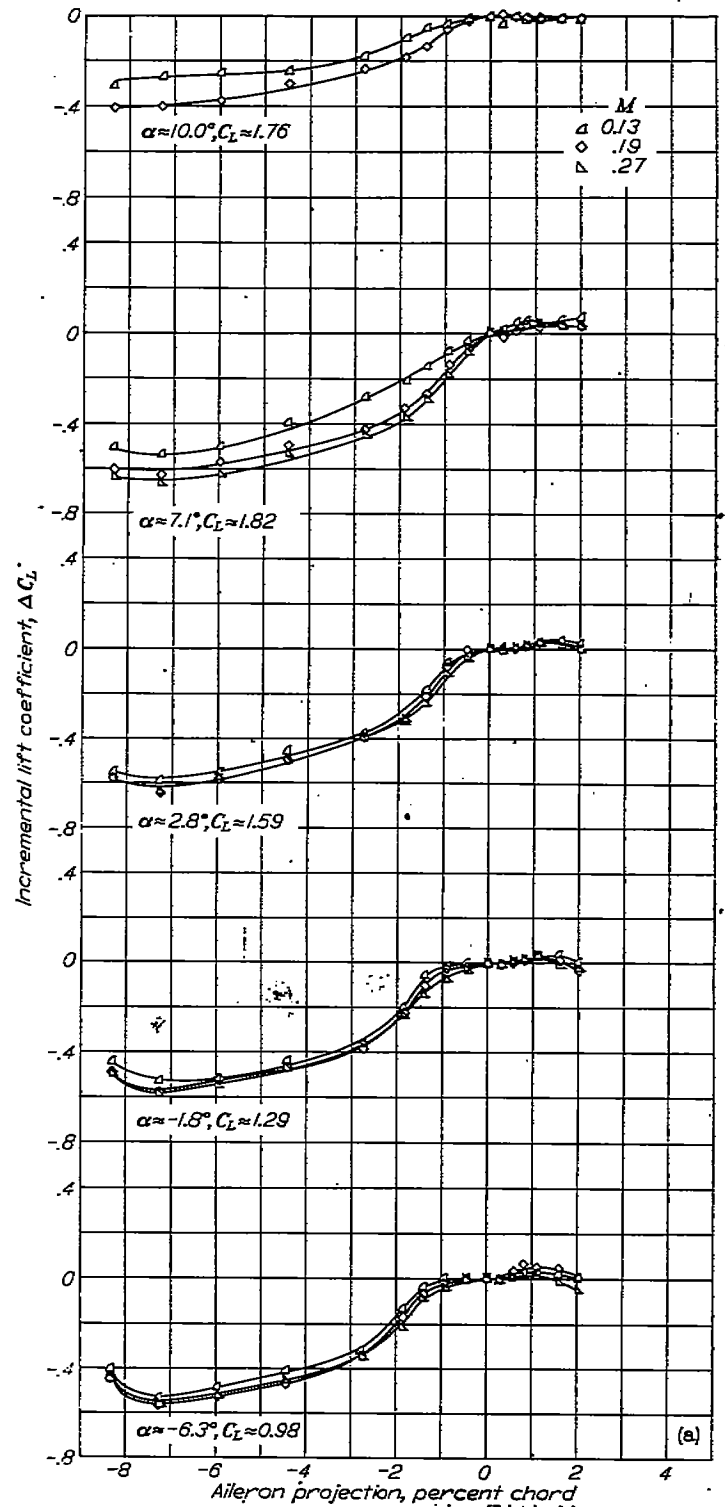
FIGURE 9.—Incremental values of lift, drag, and pitching-moment coefficients obtained by projection of the basic plug aileron on both semispans of the NACA 65-210 wing. Flap deflected 45°.
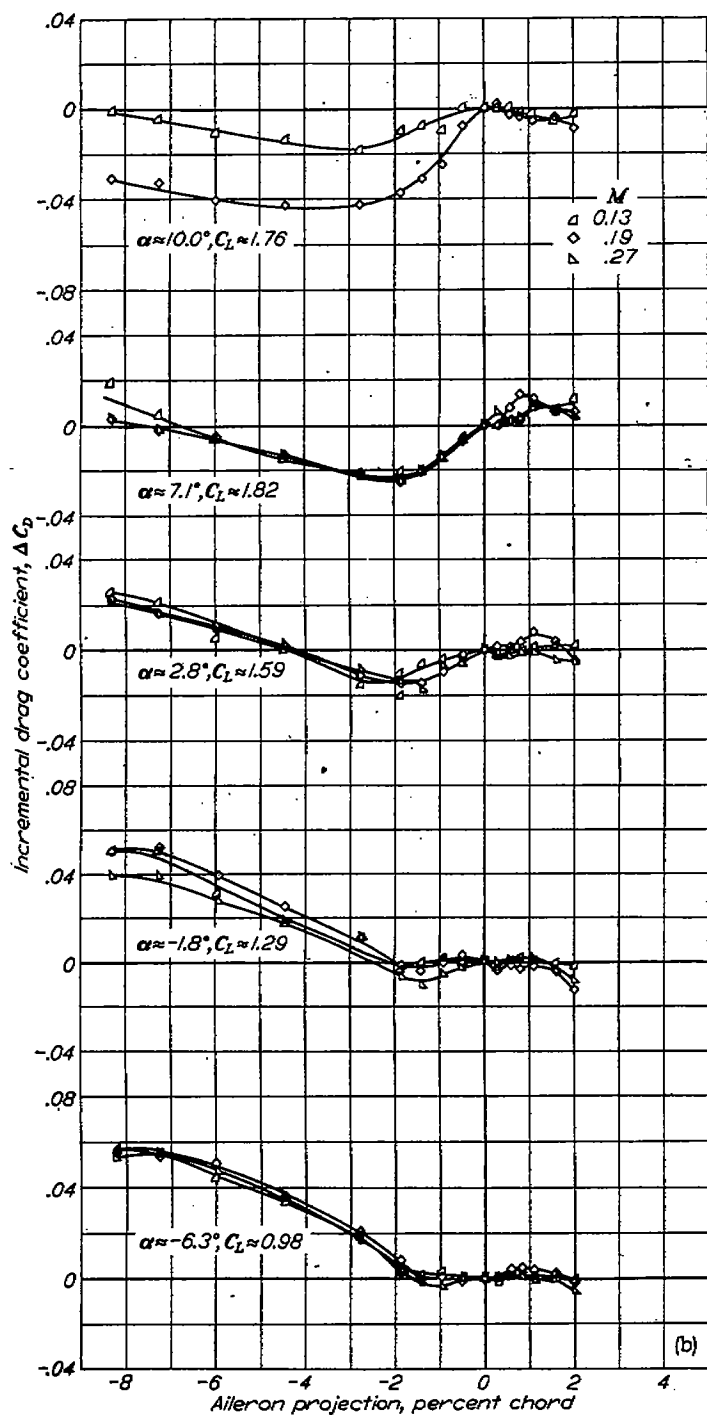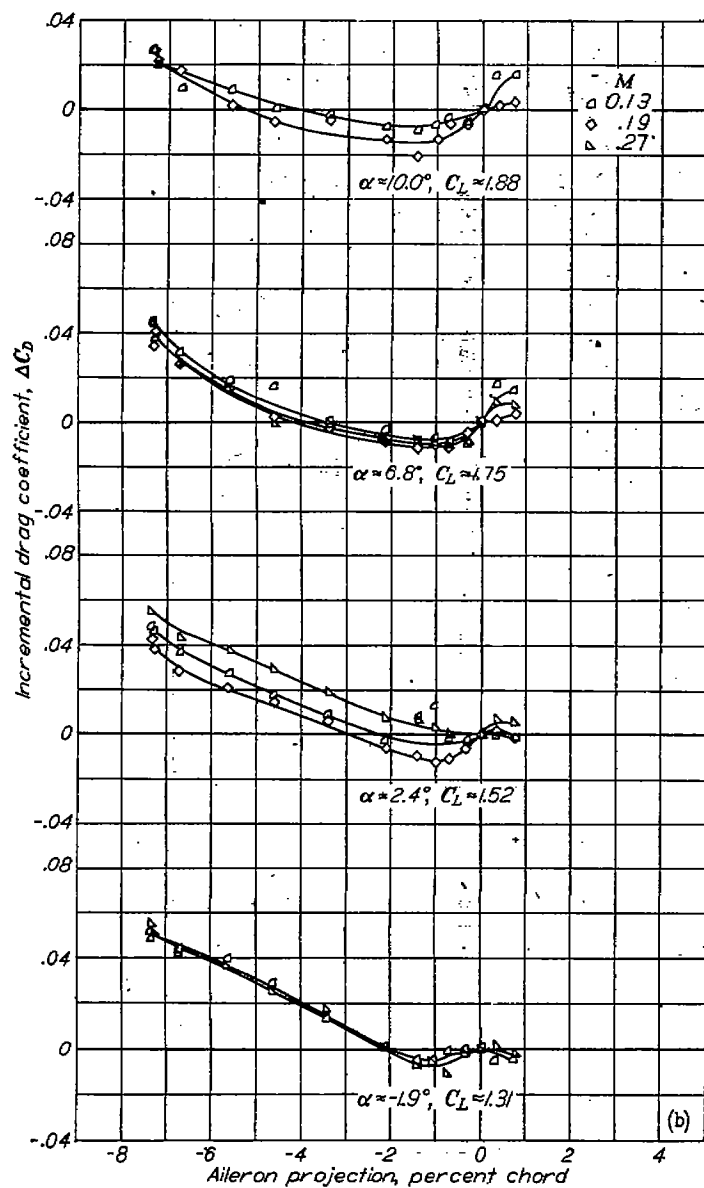
FIGURE 9—Continued.
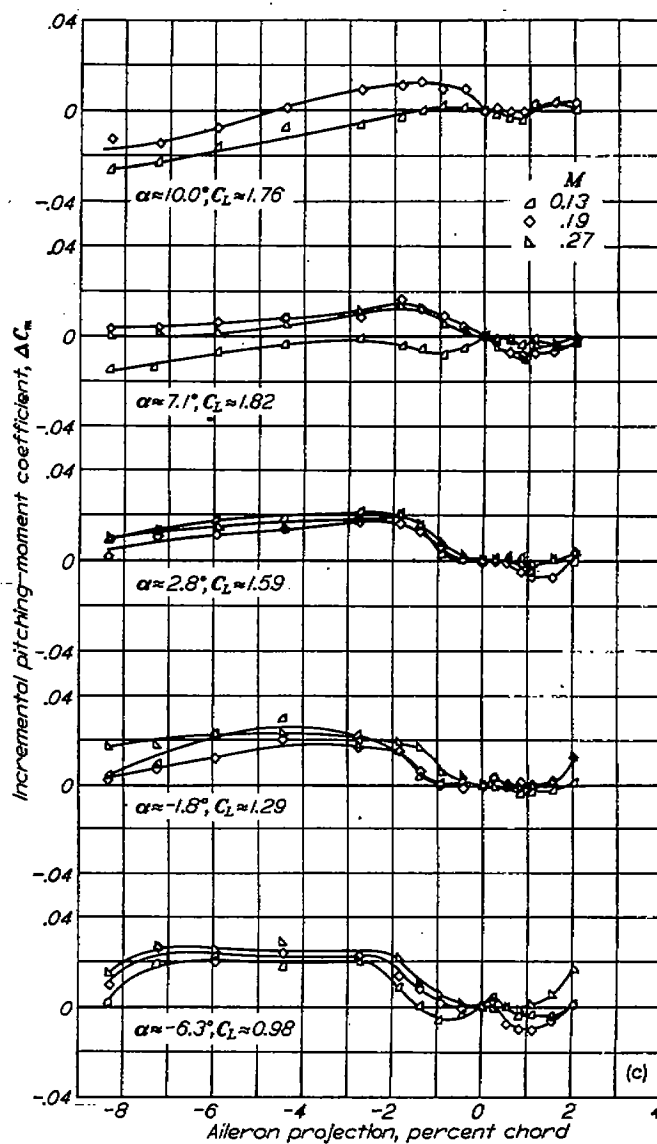
FIGURE 9.—Concluded.
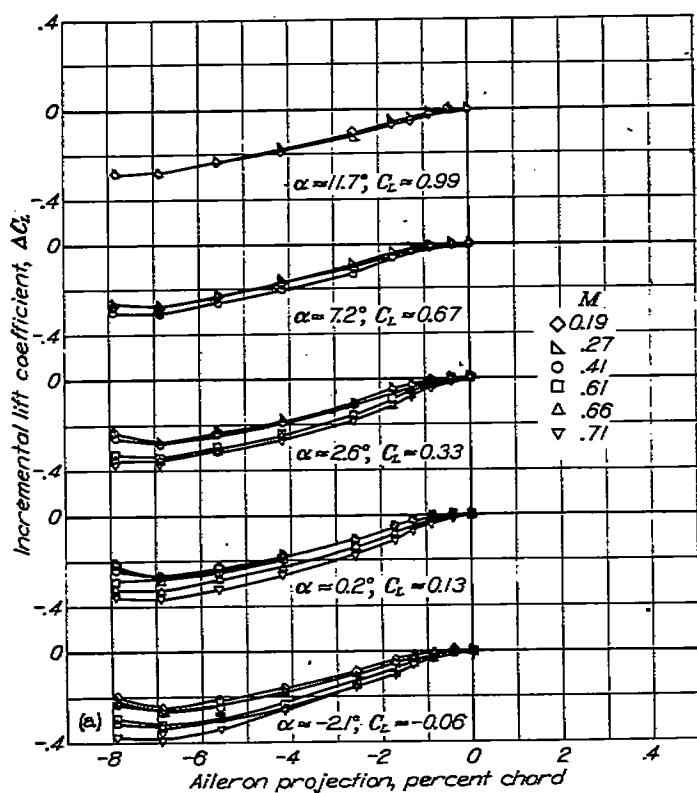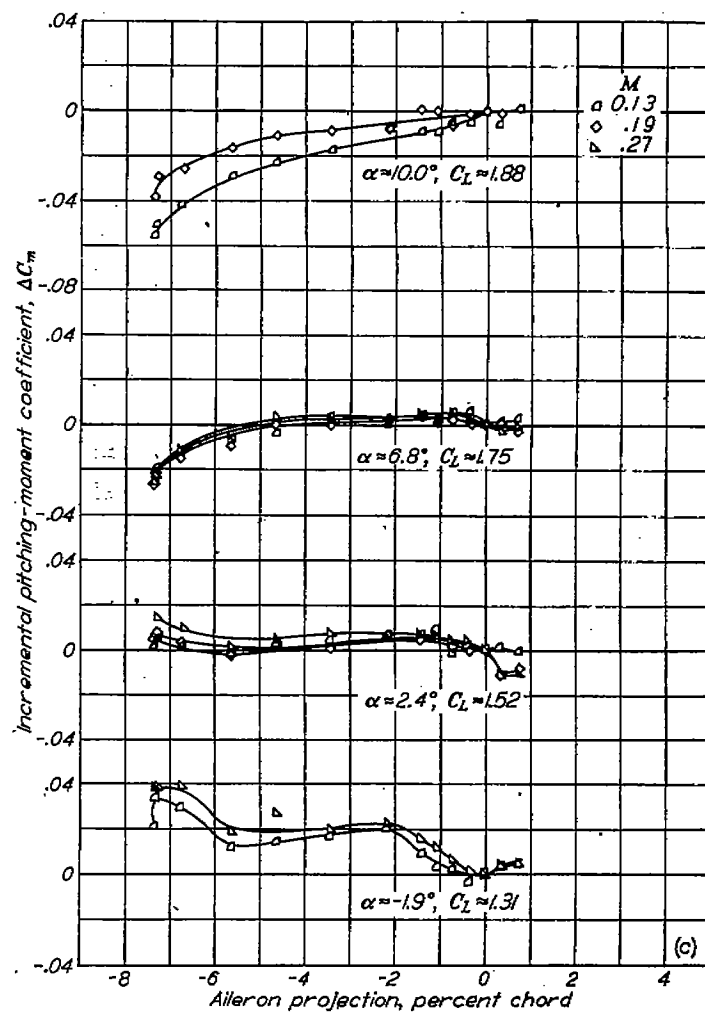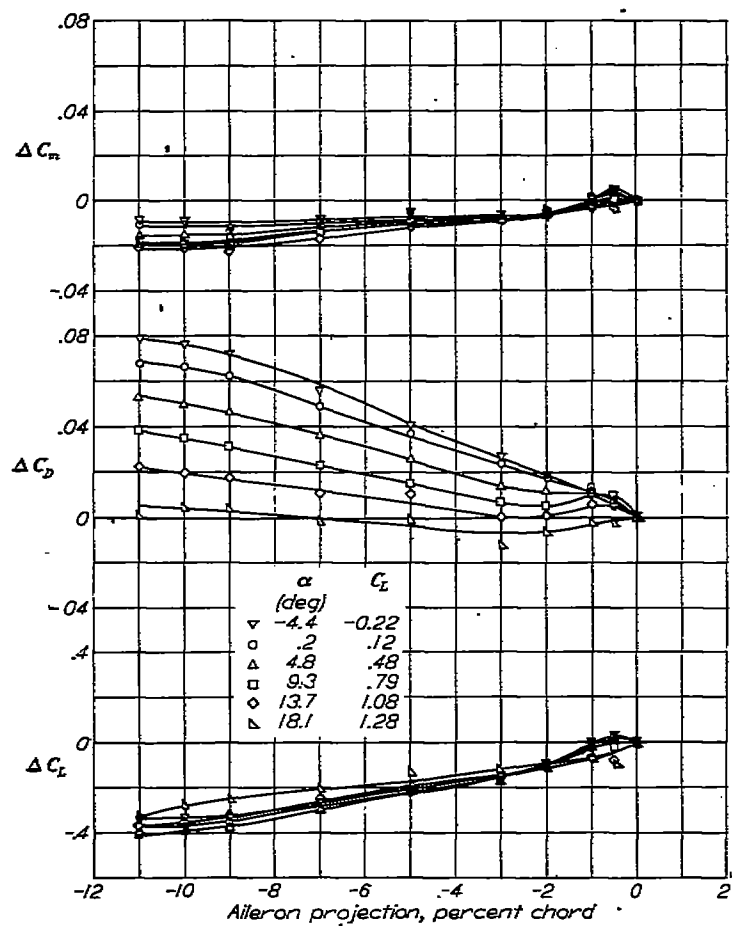
FIGURE 10.—Incremental values of lift, drag, and pitching-moment coefficients obtained by projection of the basic retractable aileron on both semispans of the NACA 65–210 wing. Flap retracted.
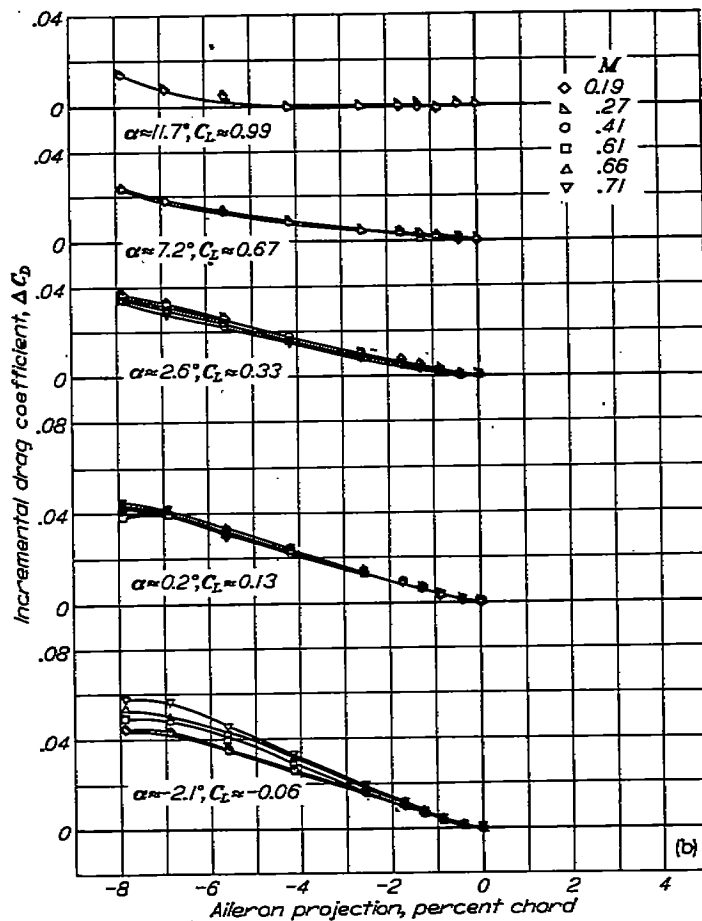
FIGURE 10.—Continued
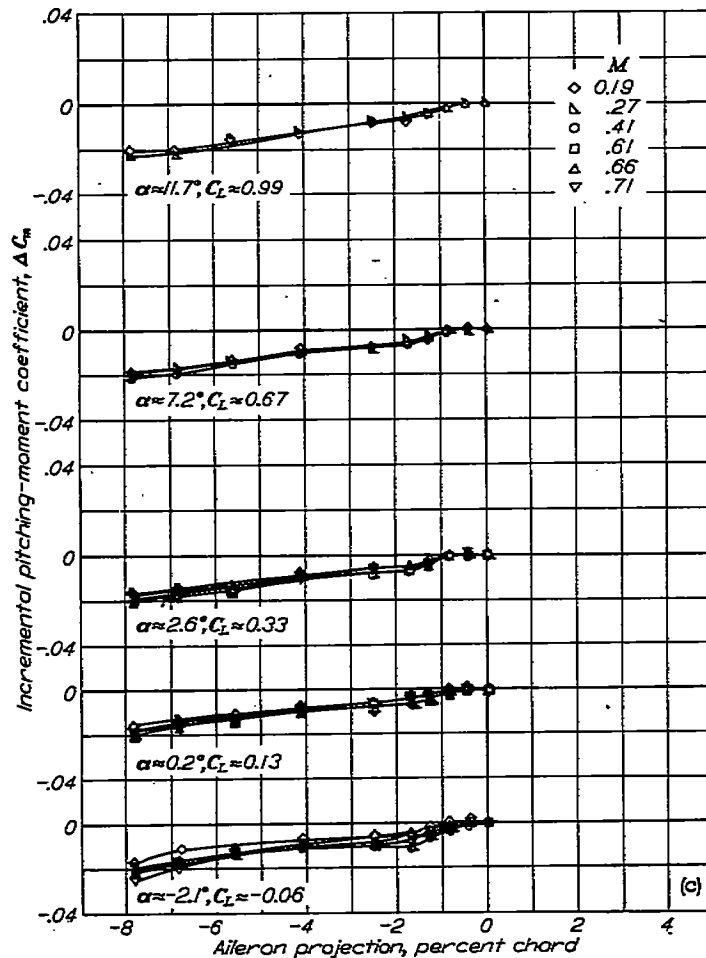
FIGURE 10.—Concluded.

FIGURE 11.—Incremental values of lift, drag, and pitching-moment coefficients obtained by projection of the basic retractable aileron on both semispans of the NACA 65–210 wing. Flap deflected 45°.
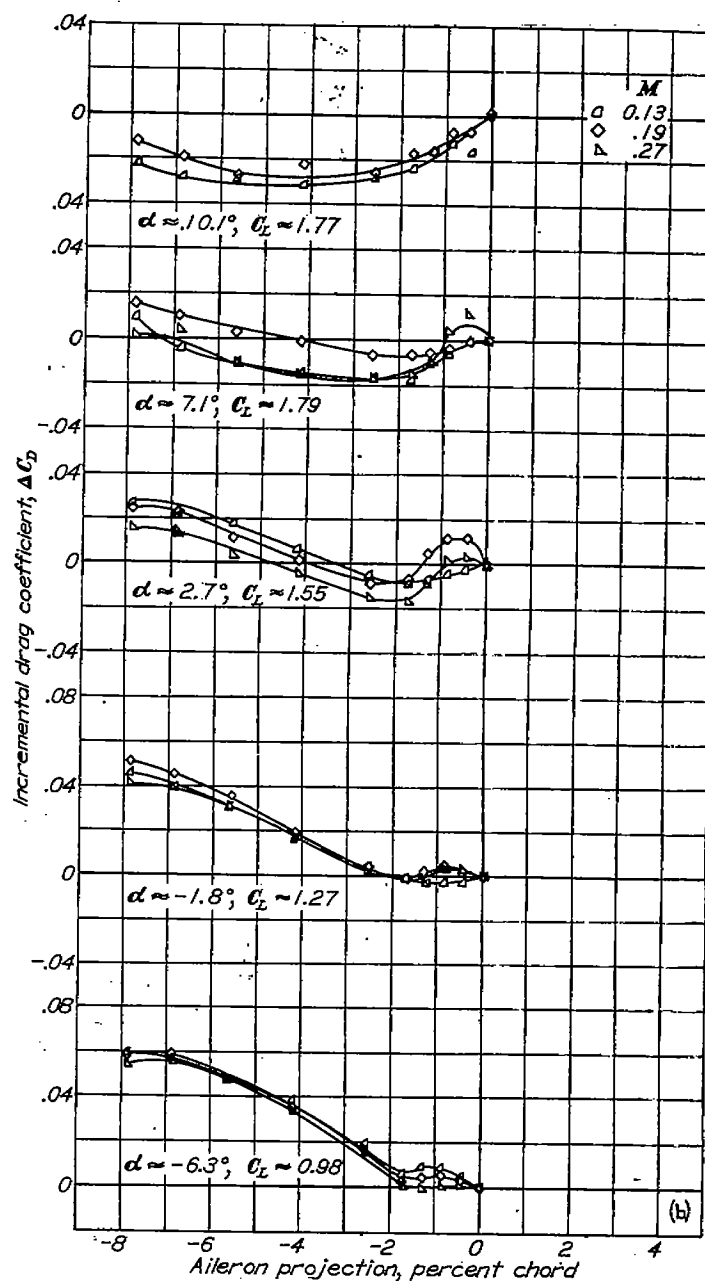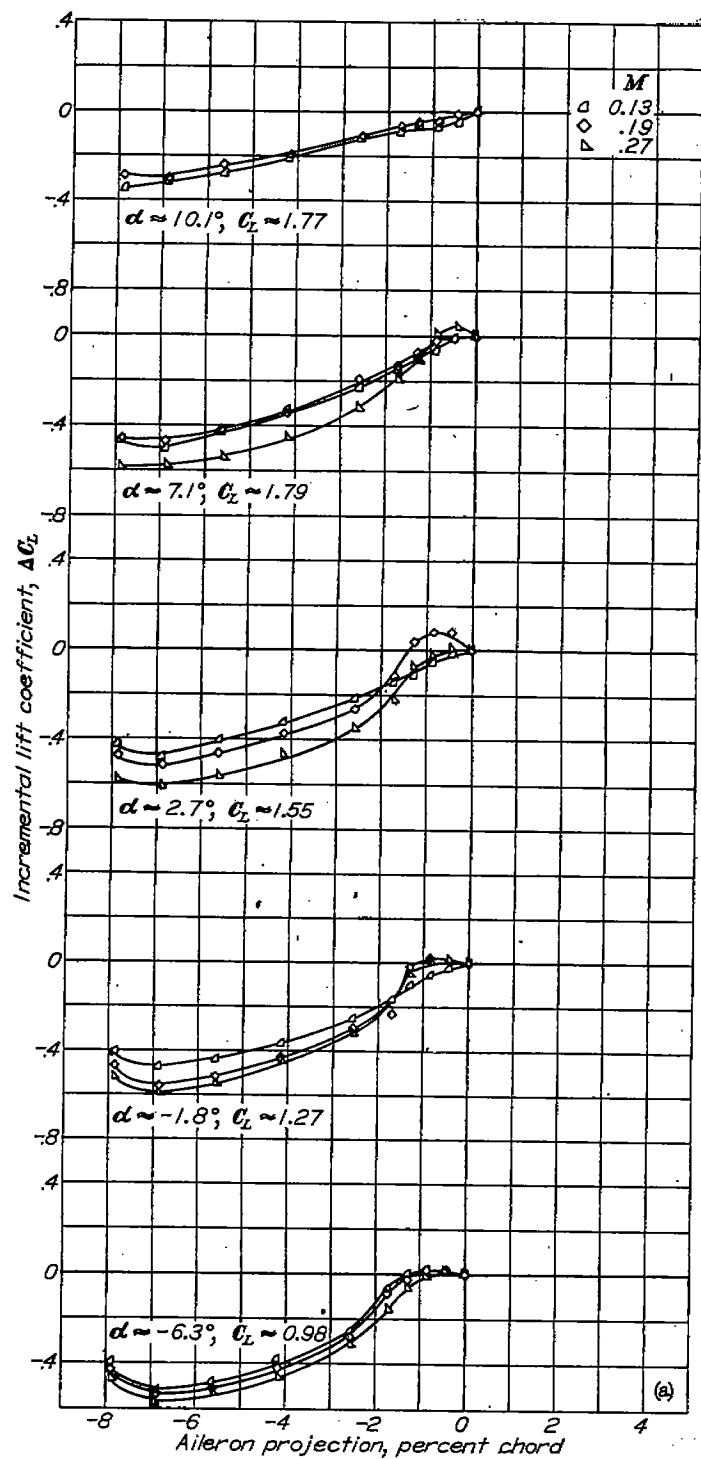
FIGURE 11.—Continued
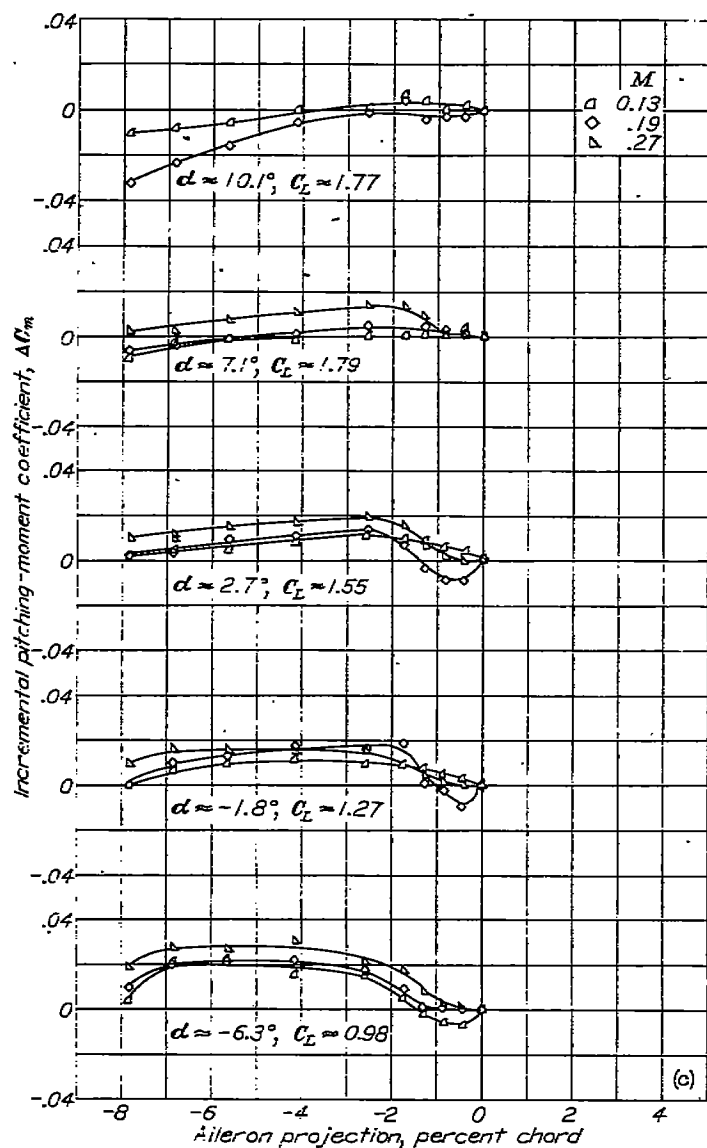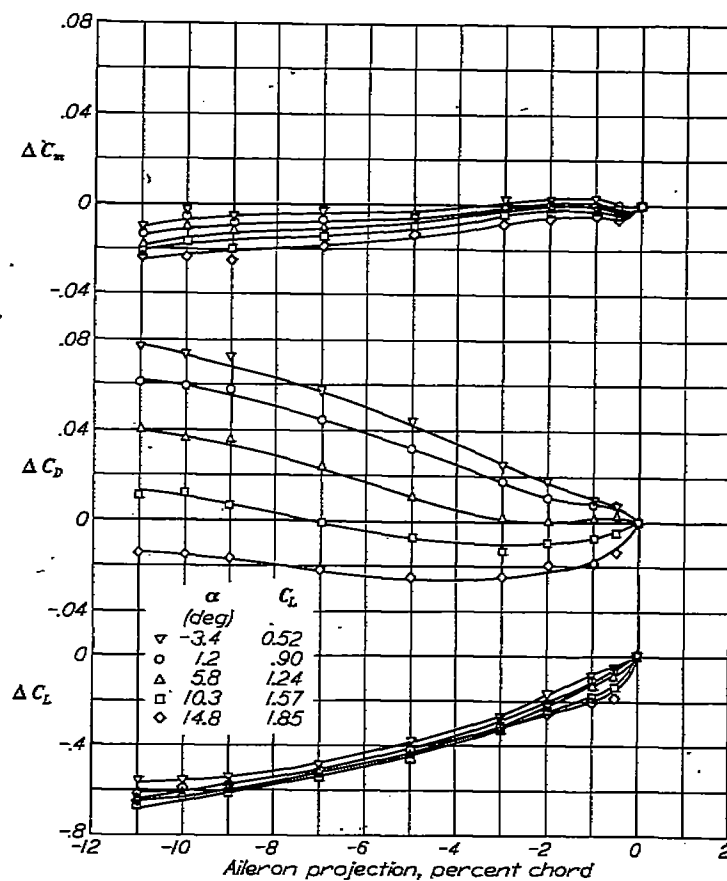
FIGURE 11.—Concluded.
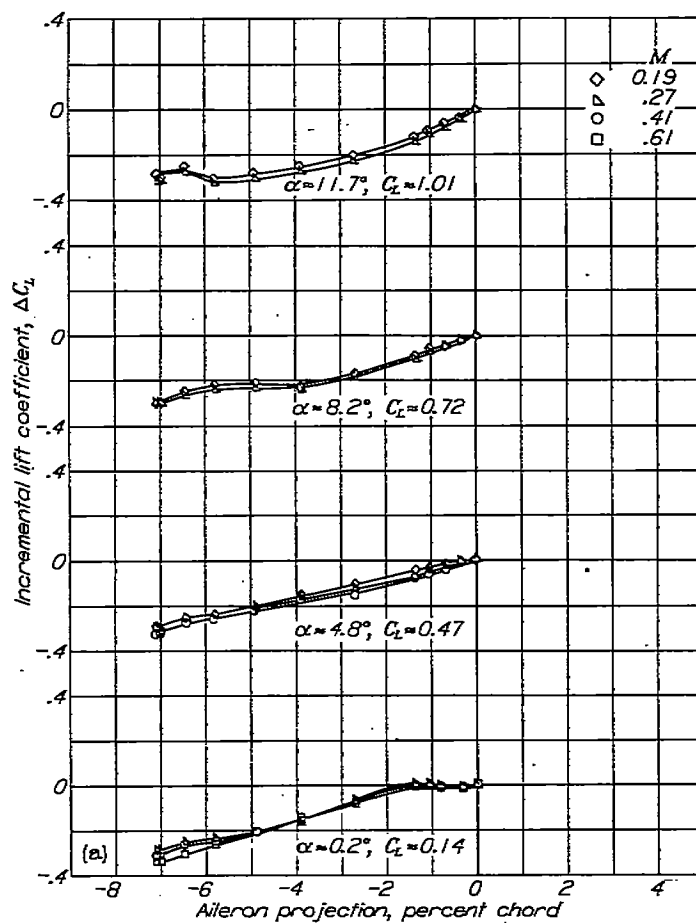
FIGURE 12.—Incremental values of lift, drag, and pitching-moment coefficients obtained by projection of the thin-plate circular plug aileron on both semispans of the NACA 65-210 wing. Flap retracted.
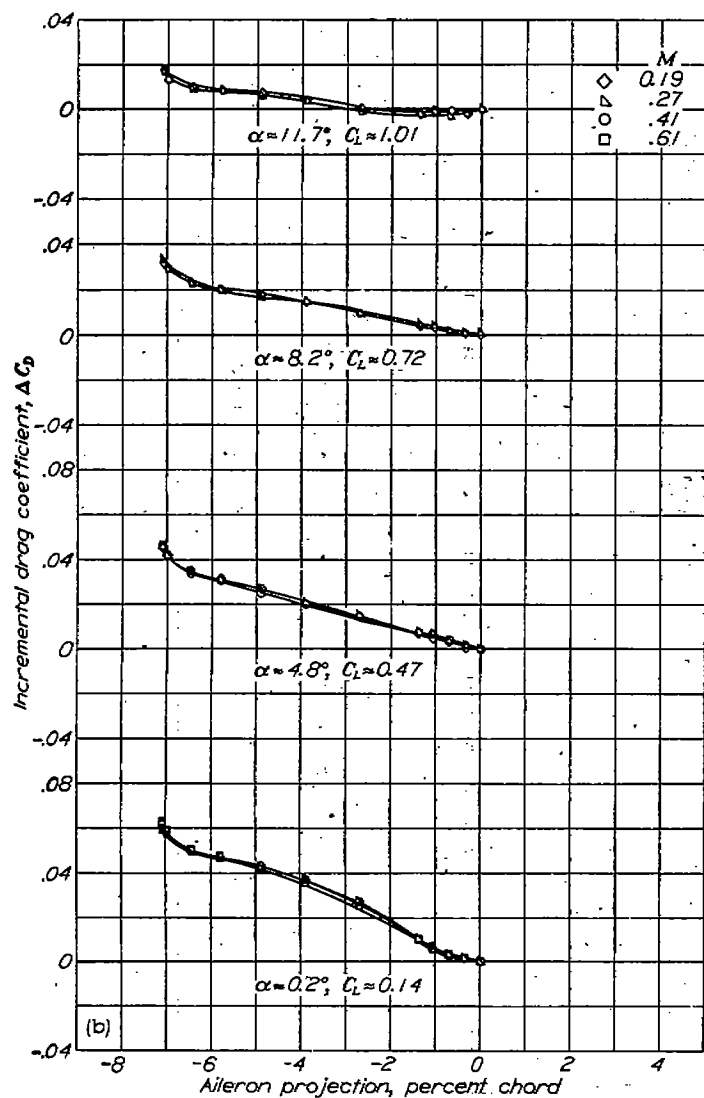
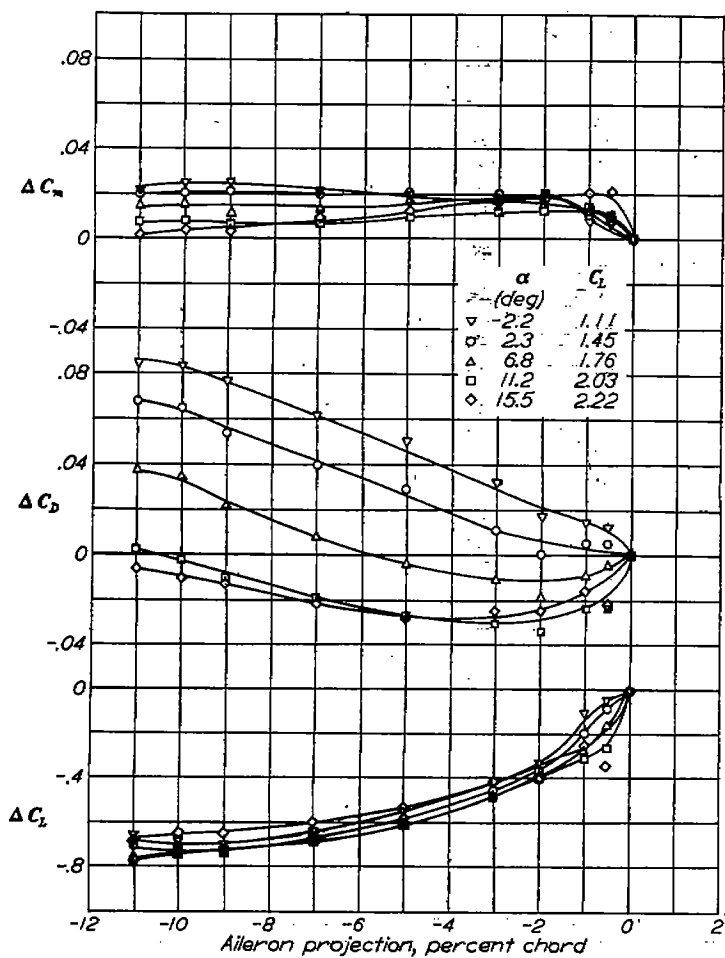FIGURE 12.—Continued.
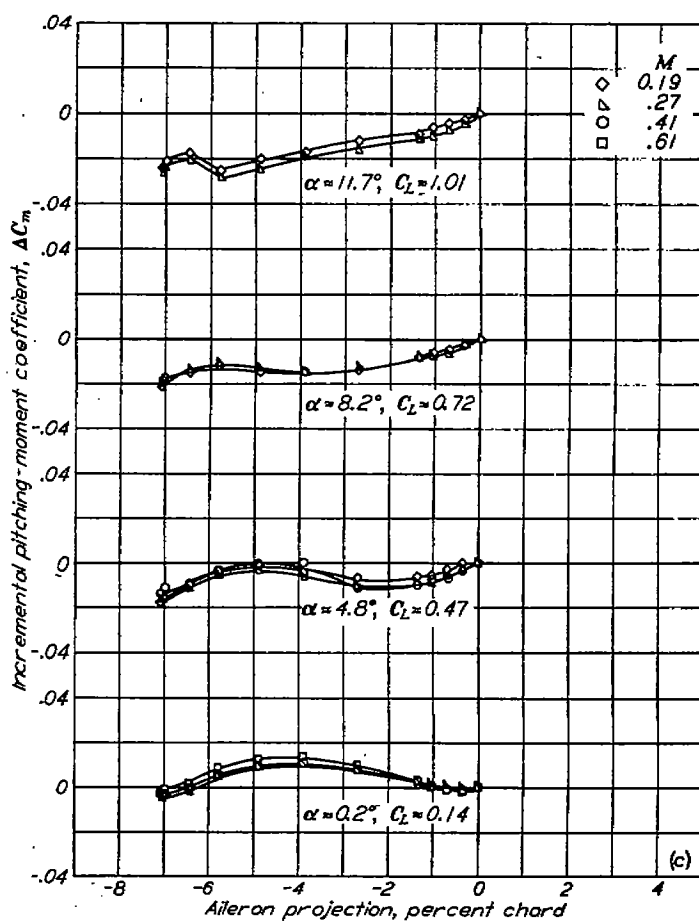
FIGURE 12.—Concluded.

FIGURE 13.—Incremental values of lift, drag, and pitching-moment coefficients obtained by projection of the thin-plate circular plug aileron on both semispans of the NACA 65–210 wing. Flap deflected 45°.
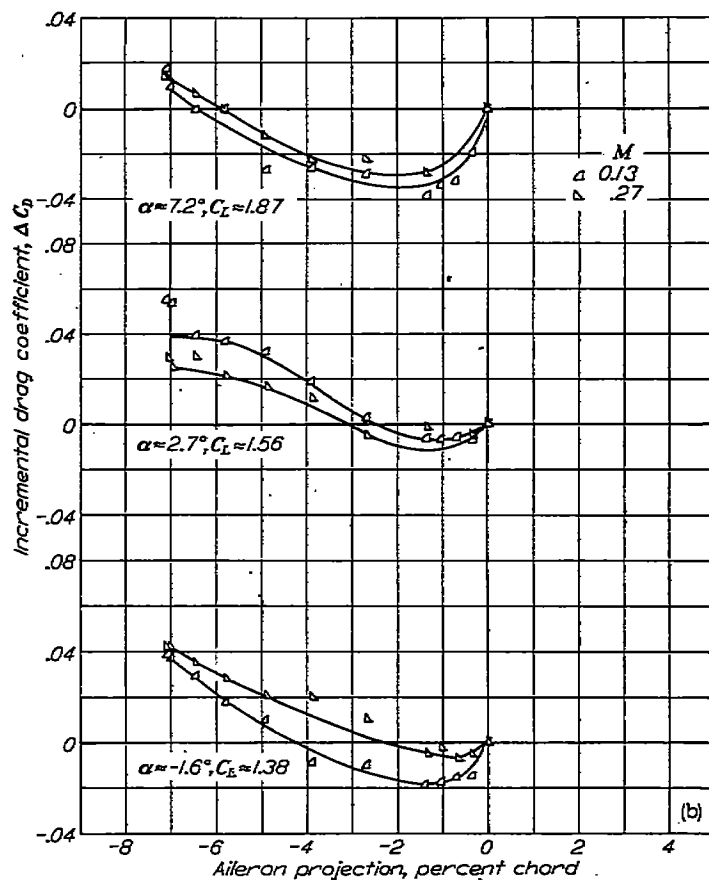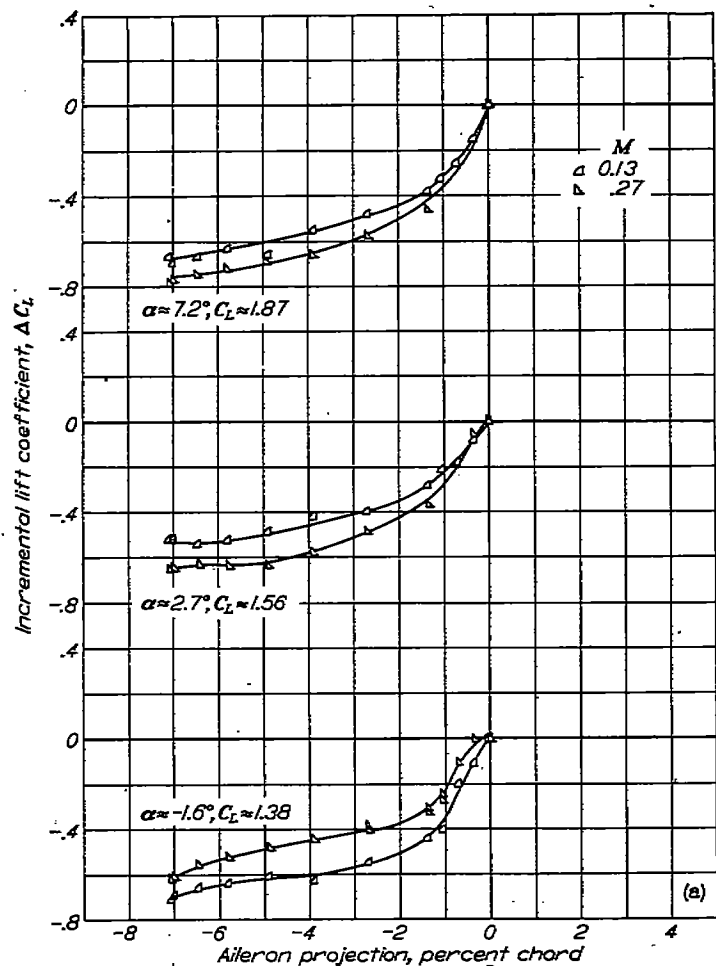
FIGURE 13.—Continued.
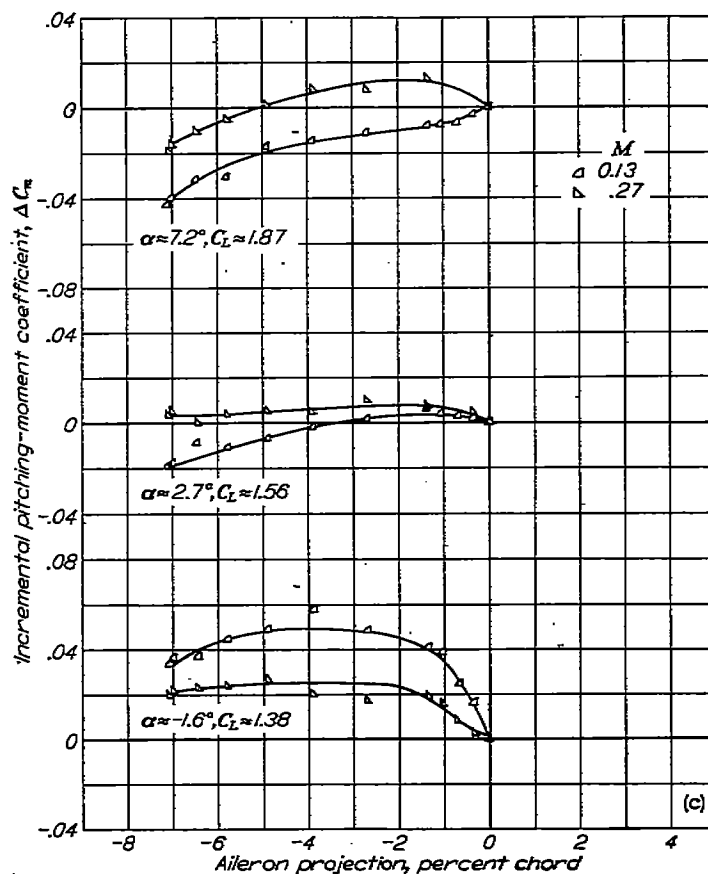
FIGURE 13.—Concluded.
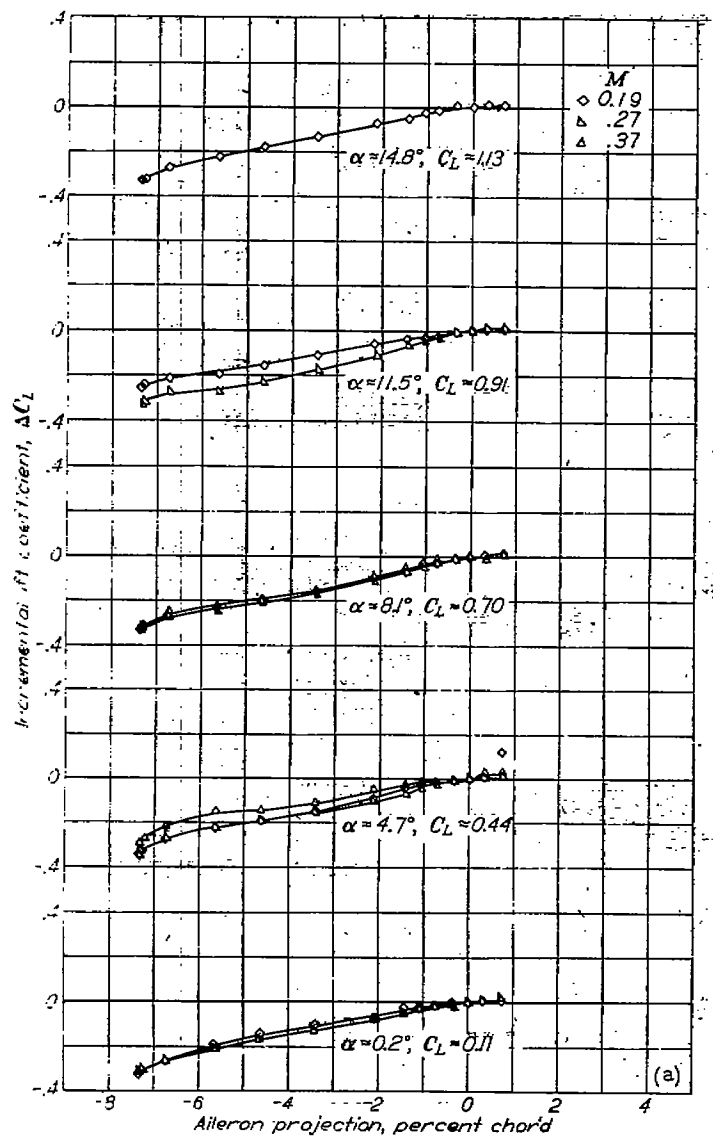
FIGURE 14.—Incremental values of lift, drag, and pitching-moment coefficients obtained by projection of the double-wall circular plug aileron on both semispans of the NACA 65–210 wing.   Flap retracted.

FIGURE 14—Continued.

FIGURE 14.—Concluded.

FIGURE 15.—Incremental values of lift, drag, and pitching-moment coefficients obtained by projection of the double-wall circular plug aileron on both semispans of the NACA 65-210 wing. Flap deflected 45°.

FIGURE 15.—Continued.
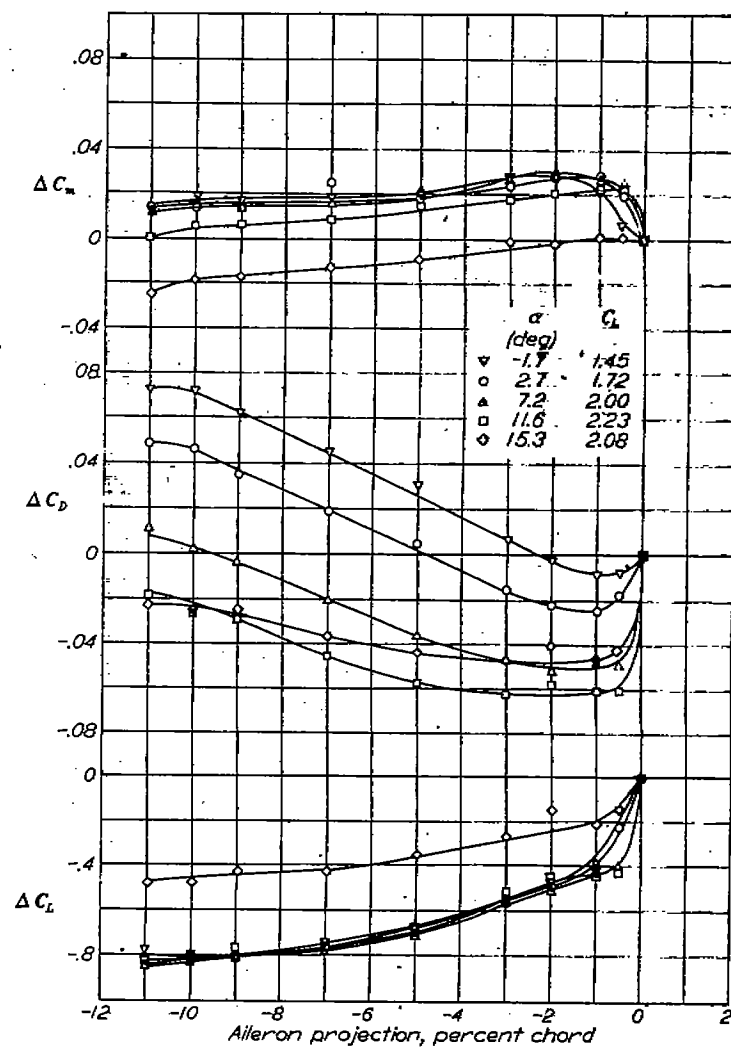
FIGURE 15.—Concluded.

FIGURE 16.—Incremental values of lift, drag, and pitching-moment coefficients obtained by projection of the plug aileron on both semispans of the NACA 65₁-215 wing. Plain wing; M=0.19.

FIGURE 17.—Incremental values of lift, drag, and pitching-moment coefficients obtained by projection of the plug aileron on both semispans of the NACA 65₁-215 wing. Flap deflected 15°; M=0.18.
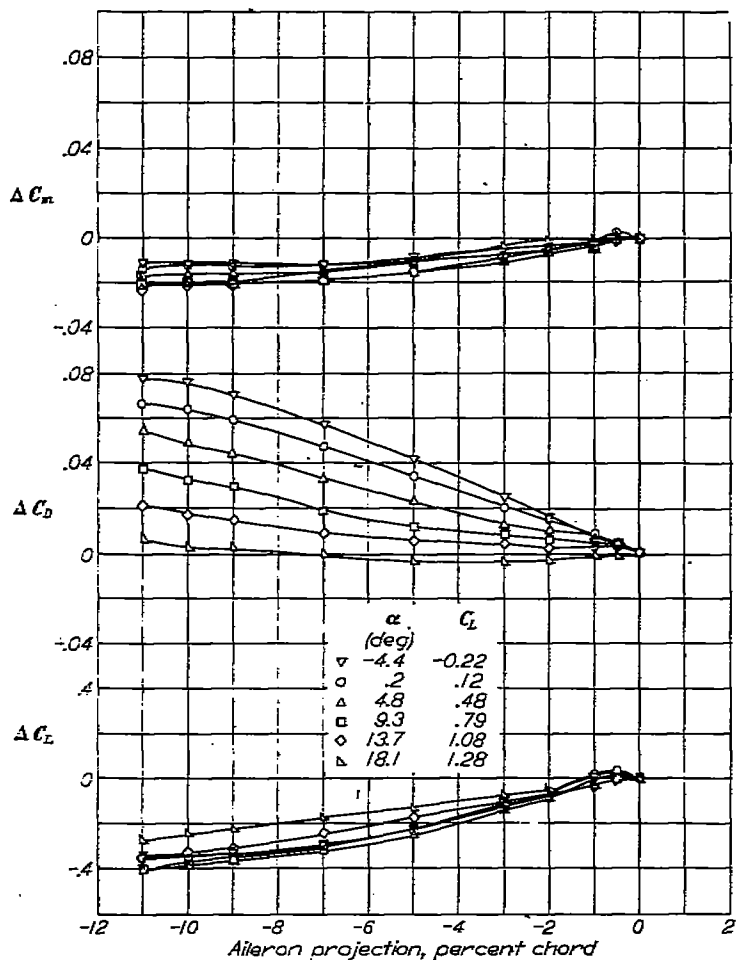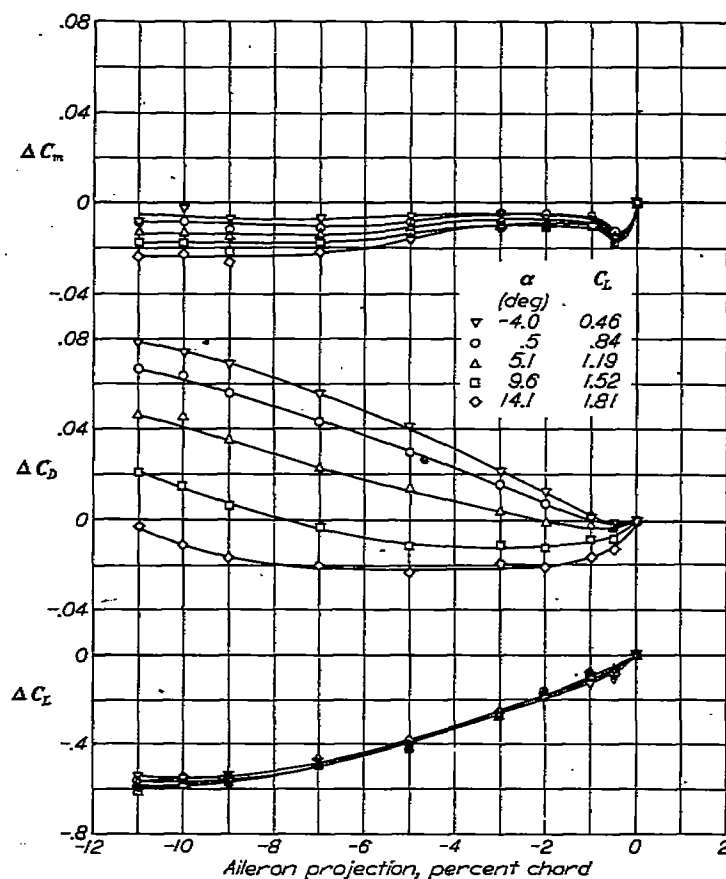
FIGURE 18.—Incremental values of lift, drag, and pitching-moment coefficients obtained by projection of the plug aileron on both semispans of the NACA 65₁-215 wing. Flap deflected 30°; M=0.13.

FIGURE 19.—Incremental values of lift, drag, and pitching-moment coefficients obtained by projection of the plug aileron on both semispans of the NACA 65₁-215 wing. Flap deflected 45°; M=0.13.
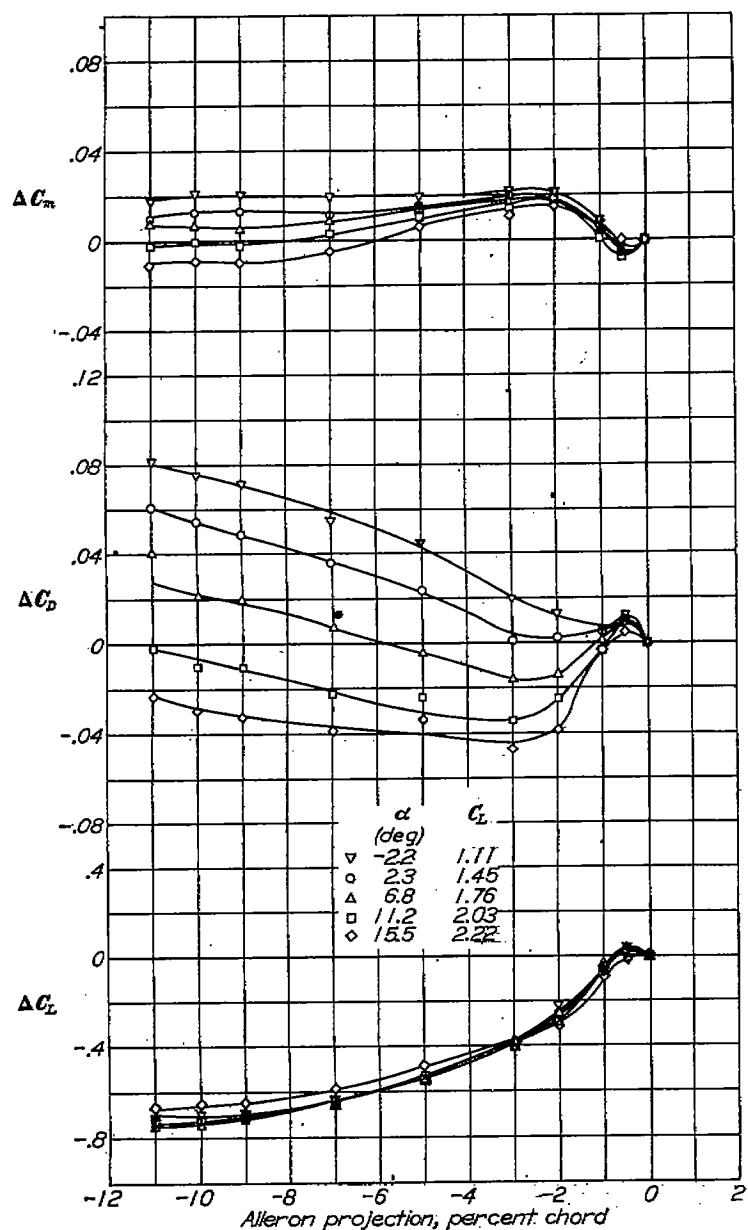
FIGURE 20.—Incremental values of lift, drag, and pitching-moment coefficients obtained by projection of the retractable aileron on both semispans of the NACA 65₂-215 wing. Plain wing; M=0.19.
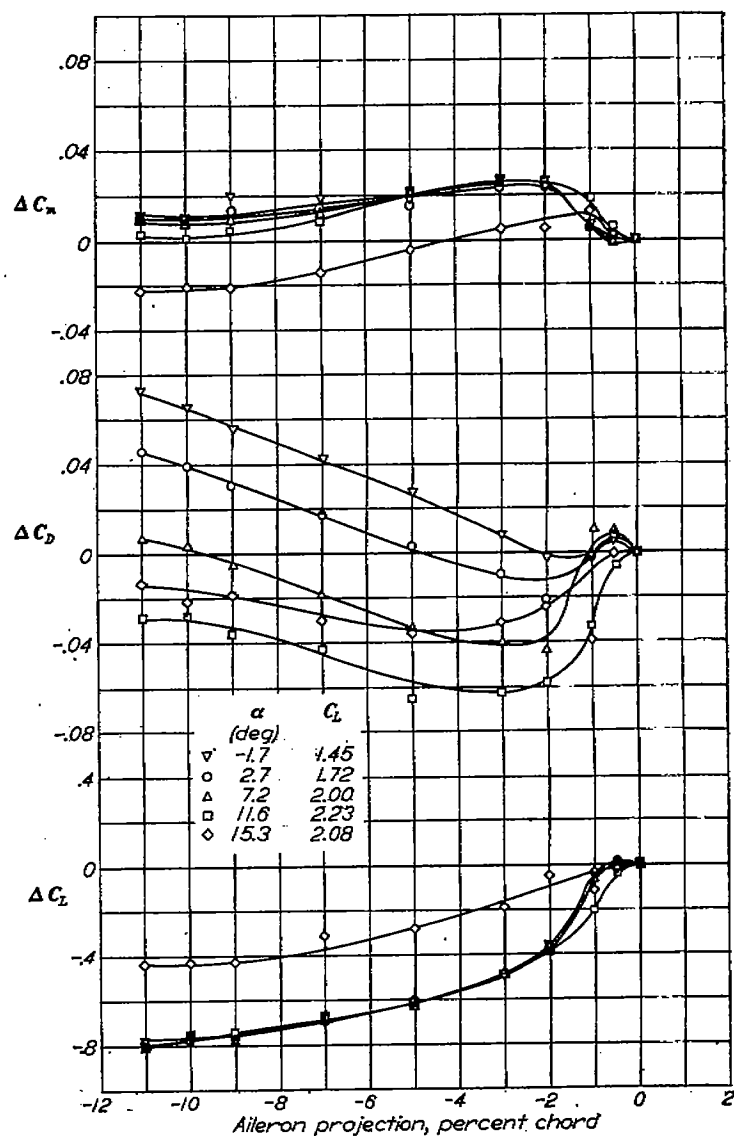
FIGURE 21.—Incremental values of lift, drag, and pitching-moment coefficients obtained by projection of the retractable aileron on both semispans of the NACA 65₂-215 wing. Flap deflected 15°; M=0.13.

FIGURE 22.—Incremental values of lift, drag, and pitching-moment coefficients obtained by projection of the retractable aileron on both semispans of the NACA 65₁-215 wing. Flap deflected 30°; M=0.13.

FIGURE 23.—Incremental values of lift, drag, and pitching-moment coefficients obtained by projection of the retractable aileron on both semispans of the NACA 65₁-215 wing. Flap deflected 45°; M=0.13.
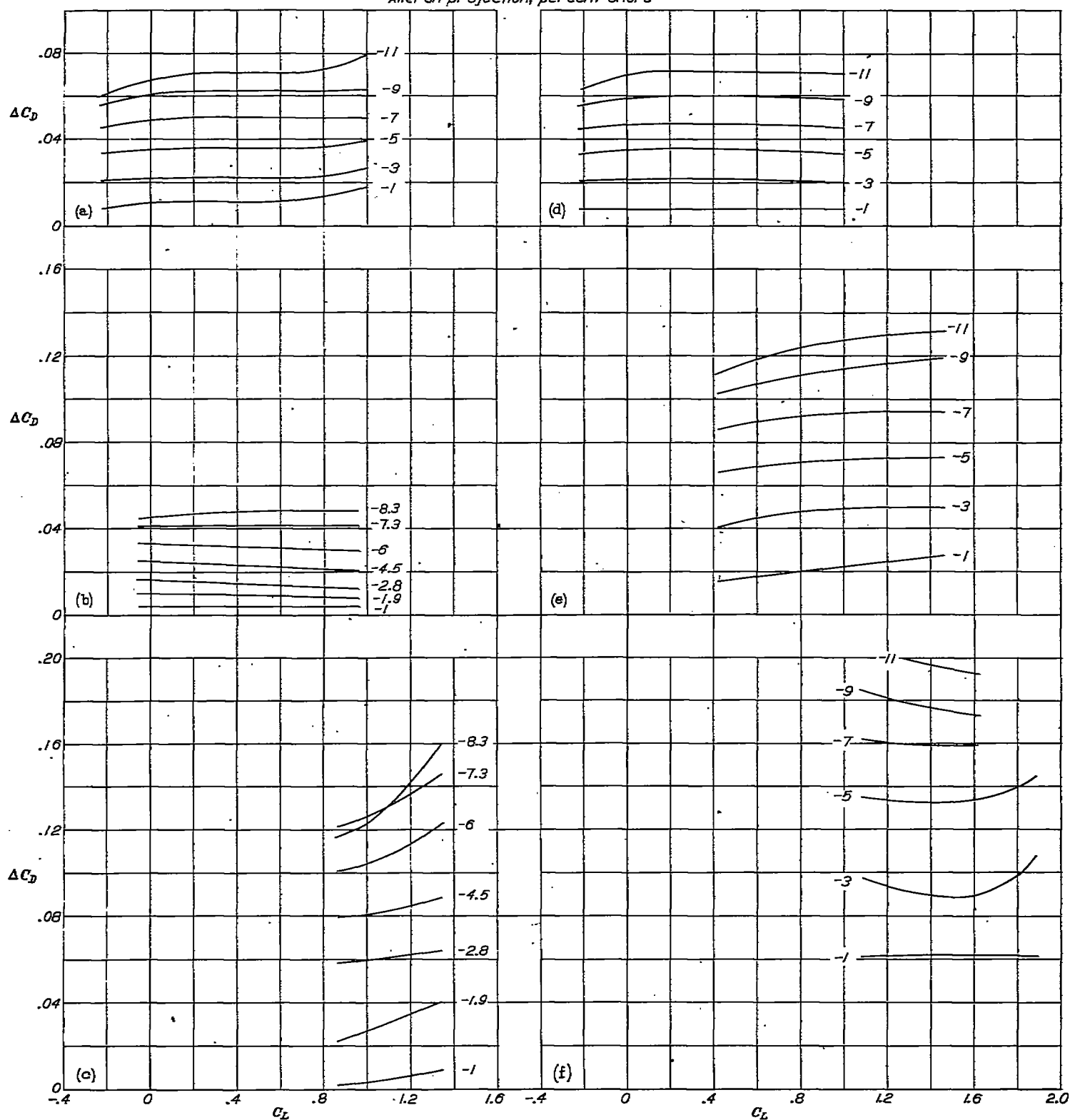
(a) Plug aileron on NACA 65₂-215 wing.
    Plain wing; $M=0.19$.
(b) Basic plug aileron on NACA 65-210
    wing. $\delta_f=0°$; $M=0.27$.
(c) Basic plug aileron on NACA 65-210
    wing. $\delta_f=45°$; $M=0.13$.

(d) Retractable aileron on NACA 65₂-215
    wing. Plain wing; $M=0.19$.
(e) Plug aileron on NACA 65₂-215 wing.
    $\delta_f=15°$; $M=0.13$.
(f) Plug aileron on NACA 65₂-215 wing.
    $\delta_f=45°$; $M=0.13$.

FIGURE 24.—Incremental values of drag coefficient obtained at constant lift coefficient for several of the wing aileron configurations investigated.
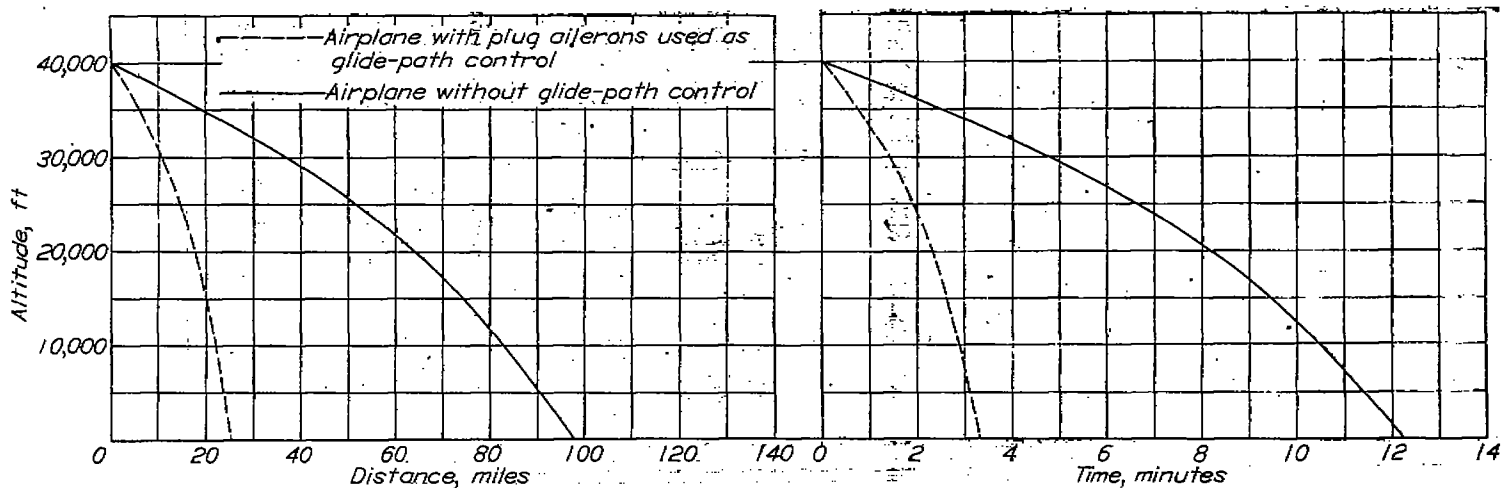
FIGURE 25.—Comparison of estimated elapsed time and ground distance covered during descent of a typical airplane from an altitude of 40,000 feet with and without a glide-path control. Plug ailerons raised to 8-percent-chord projection on both semispan wings used as glide-path control. (Assumed airplane conditions: wing loading, 63 lb/sq ft; wing aspect ratio, 10.18; wing taper ratio, 0.43; effective propeller thrust, 0; $\delta_f=0°$; $M=0.7$ until $V_i=450$ mph is attained.)
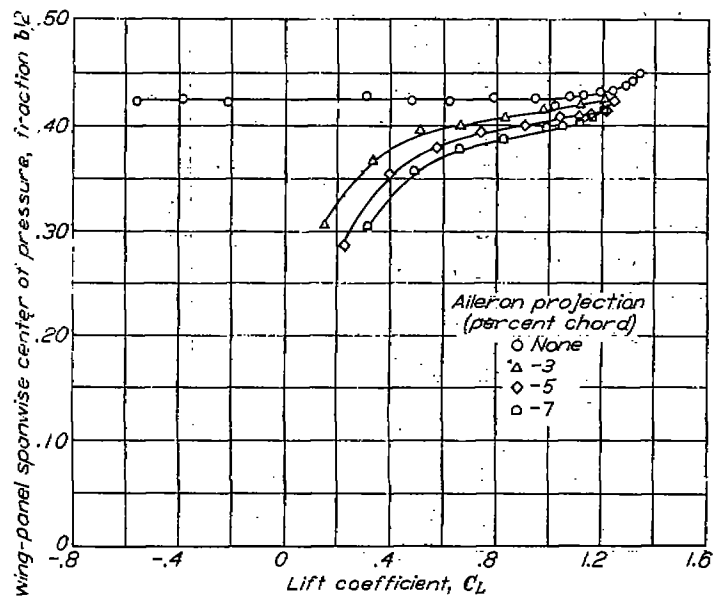

FIGURE 26.—Effect of aileron projection on wing-panel spanwise center of pressure of the NACA 65₂-215 wing with retractable ailerons. Plain wing; $M=0.19$.

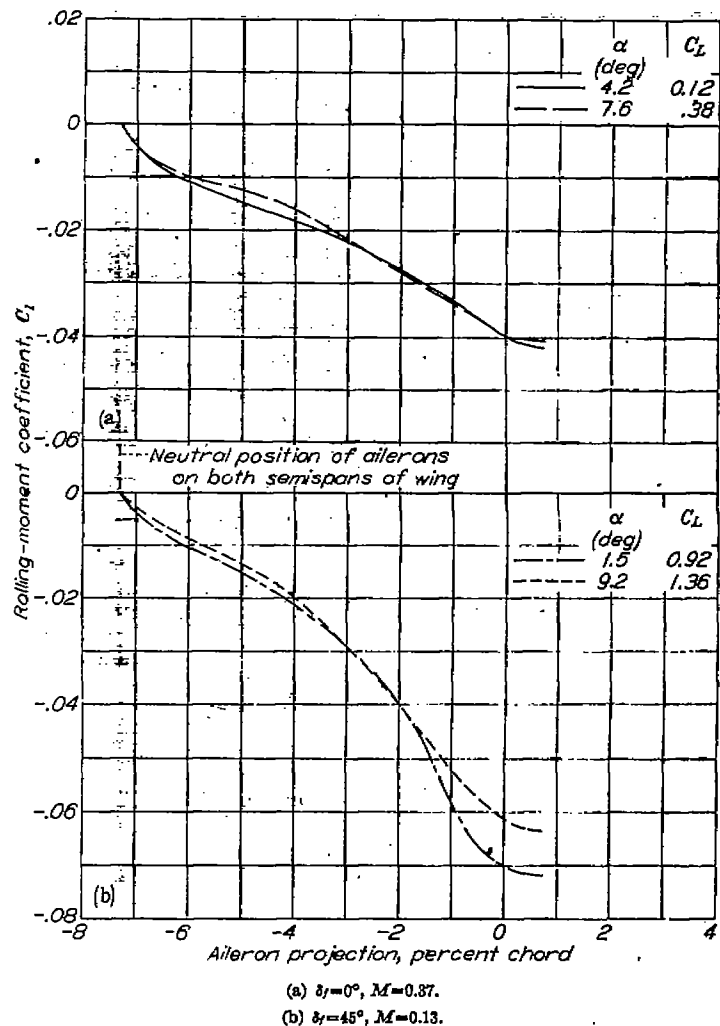(a) $\delta_f=0°$, $M=0.37$.

(b) $\delta_f=45°$, $M=0.13$.

FIGURE 27.—Variation of rolling-moment coefficient of complete wing with projection of double-wall circular plug aileron on one semispan of NACA 65-210 wing. Neutral position of ailerons: −7.3-percent-chord projection on both semispans of a complete wing. (See reference 4.)

(a) $\delta_f = 0°$, $M = 0.41$.
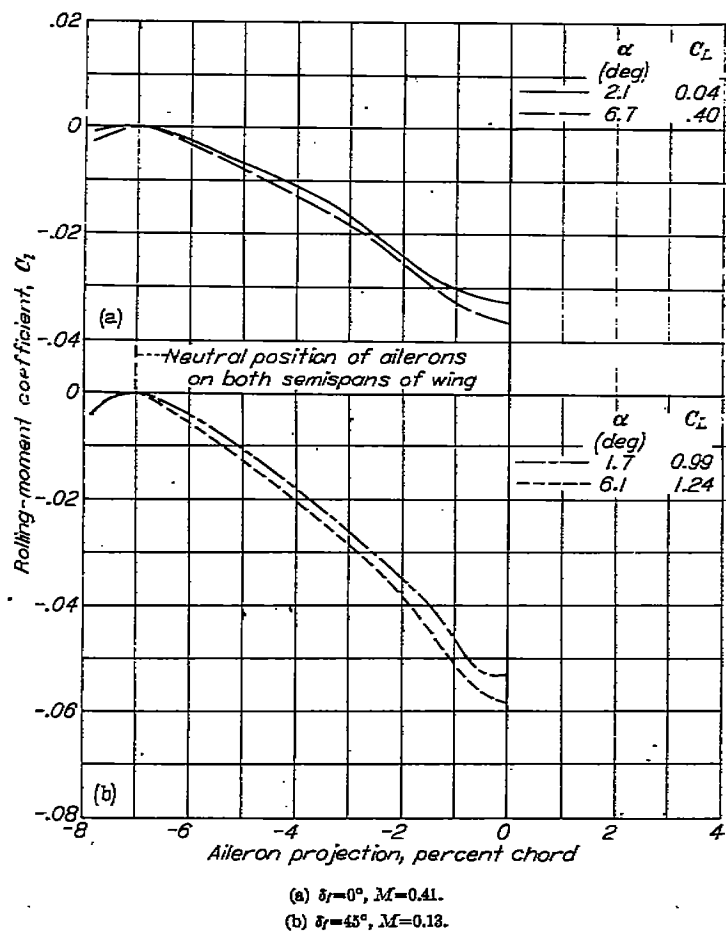
(b) $\delta_f = 45°$, $M = 0.13$.

FIGURE 28.—Variation of rolling-moment coefficient of complete wing with projection of basic retractable aileron on one semispan of NACA 65-210 wing. Neutral position of ailerons: −7.0-percent-chord projection on both semispans of a complete wing. (See reference 3.)

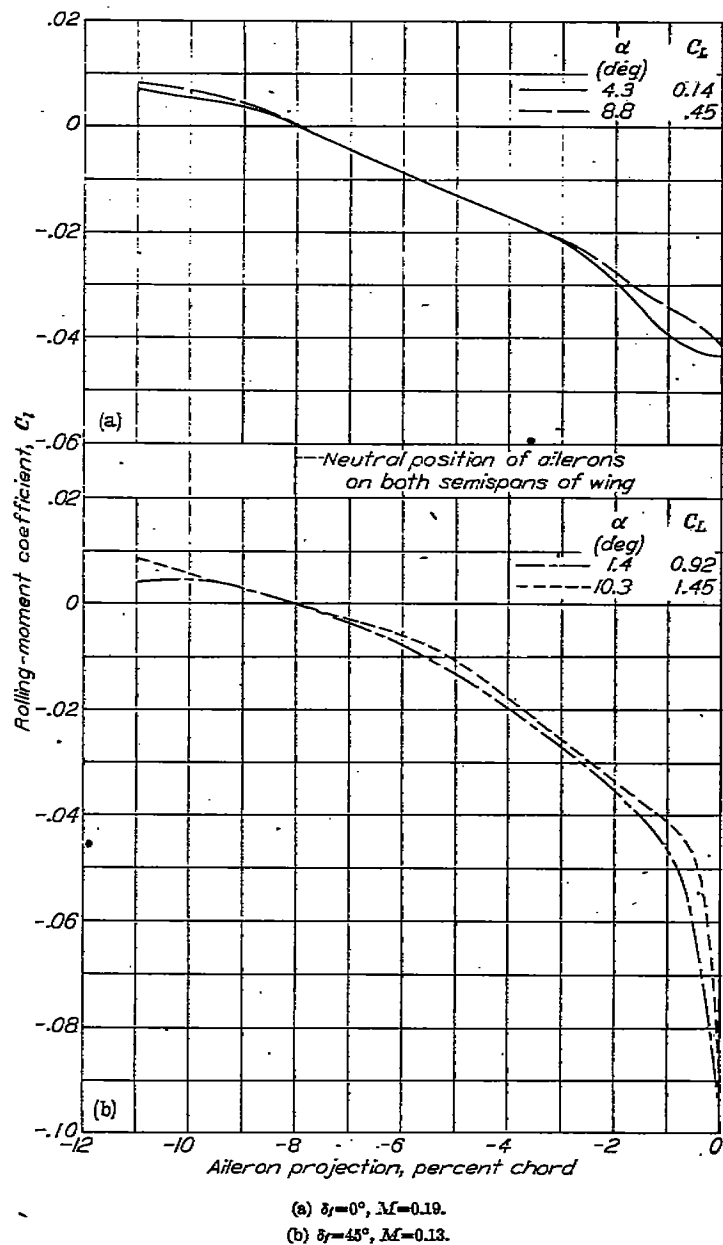(a) $\delta_f = 0°$, $M = 0.19$.

(b) $\delta_f = 45°$, $M = 0.13$.

FIGURE 29.—Variation of rolling-moment coefficient of complete wing with projection of plug aileron on one semispan of NACA 65₁-215 wing. Neutral position of ailerons: −8.0 percent-chord projection on both semispans of a complete wing. (See reference 5.)